# XRF techniques for materials and life sciences

Alessandro Migliori

Nuclear Science and Instrumentation Laboratory

International Atomic Energy Agency

# Conventional XRF

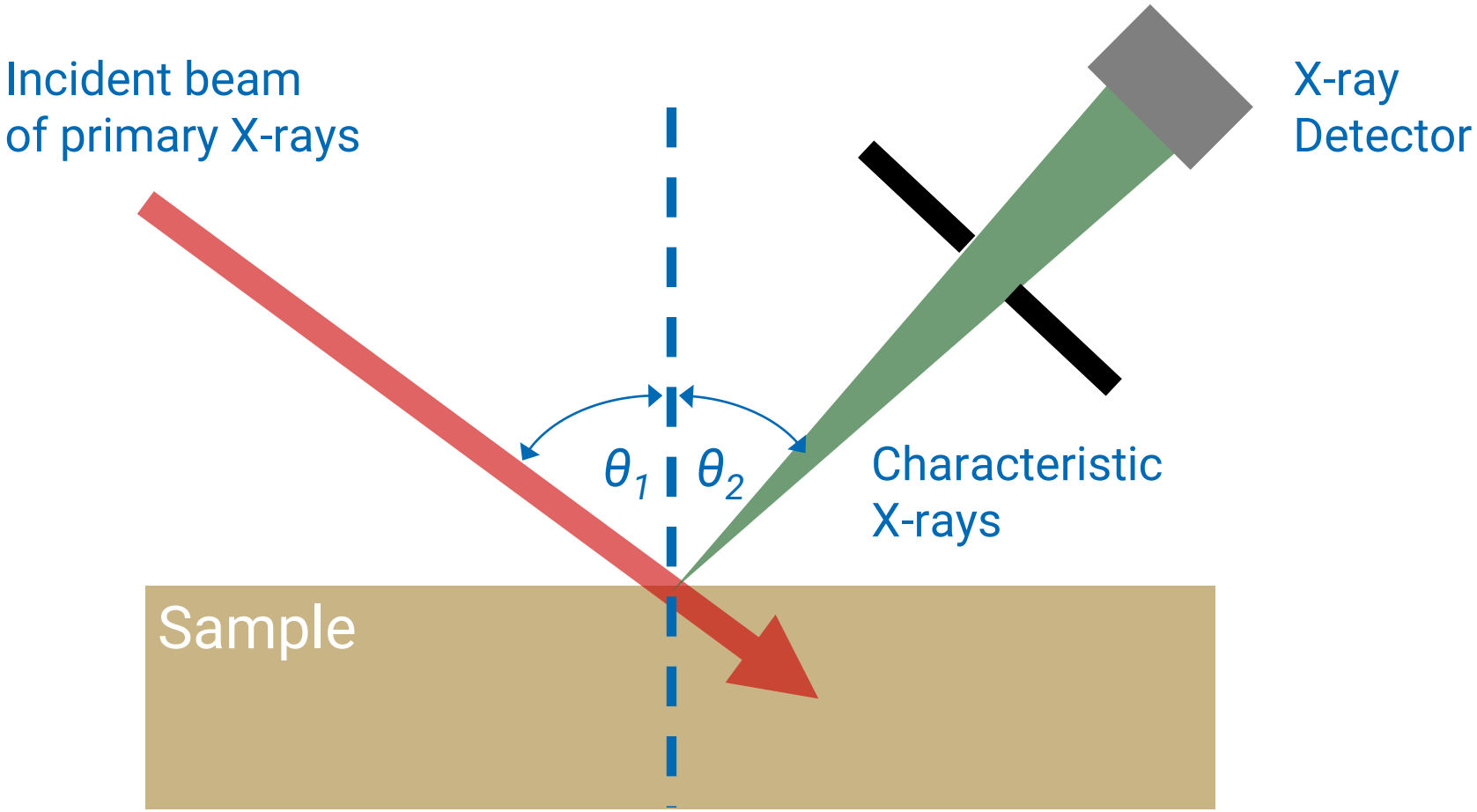

# Sources of ionizing radiation

- Electrons (SEM)
- Charged particles (accelerators)
- **Radioisotopes (α, γ, X-rays)**
- **X-ray Tubes**
- **Synchrotron radiation**

# Interaction of X-rays with matter

**X-rays can interact with the atoms of the material in two different ways:**

- **Photoelectric effect**: Primary X-ray radiation can ionise atoms of the material. The X-ray is absorbed in this process

- **Scattering**:
  - ✓ **Elastic/Coherent scattering** (**Rayleigh**): no energy loss after collision with electrons. The Rayleigh effect is present when electrons are strongly bound (inner atomic electrons)
  - ✓ **Inelastic/Incoherent scattering** (**Compton**): energy loss after collision with electrons. The Compton effect is present when electrons are loosely bound (outer, less bound electrons)

# Photoelectric effect

## Primary X-ray radiation can ionise atoms of the material to be analysed

Cross section of the PE depends strongly on Z of the material and on the energy of the primary X-ray

$$\sigma_{Ph} \propto \frac{Z^n}{E_X^{3.5}} \qquad n = 3 \div 4$$

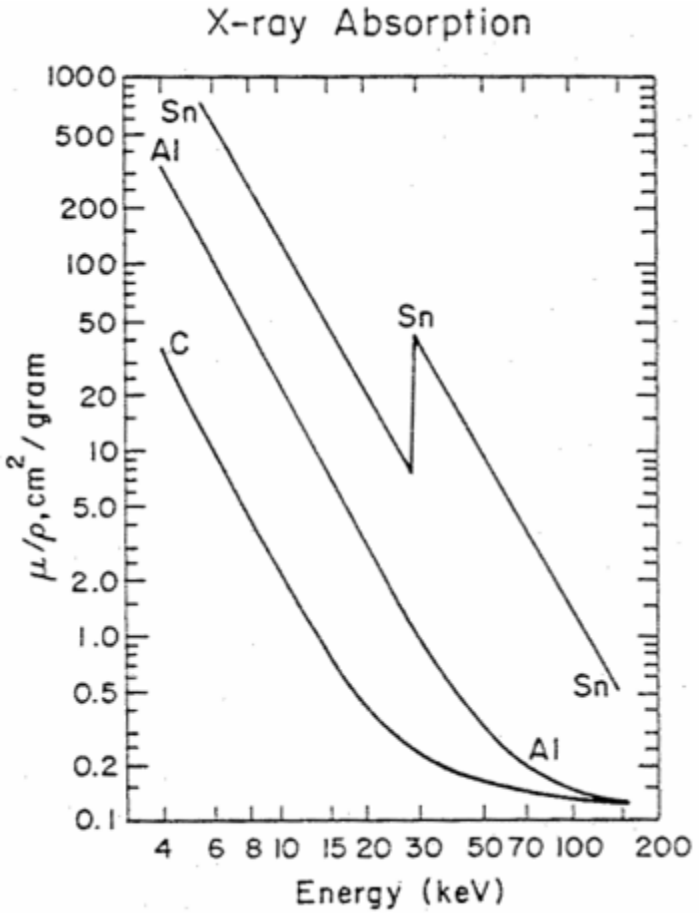


To maximize the ionization probability, the energy of the primary X-ray should be higher than the binding energy but as close as possible to it

# X-Ray Fluorescence

**Incident photon Energy $E_0$** should be adequate to ionize the atomic bound electrons
→ **$E_0$ ≥ inner shell binding energy**

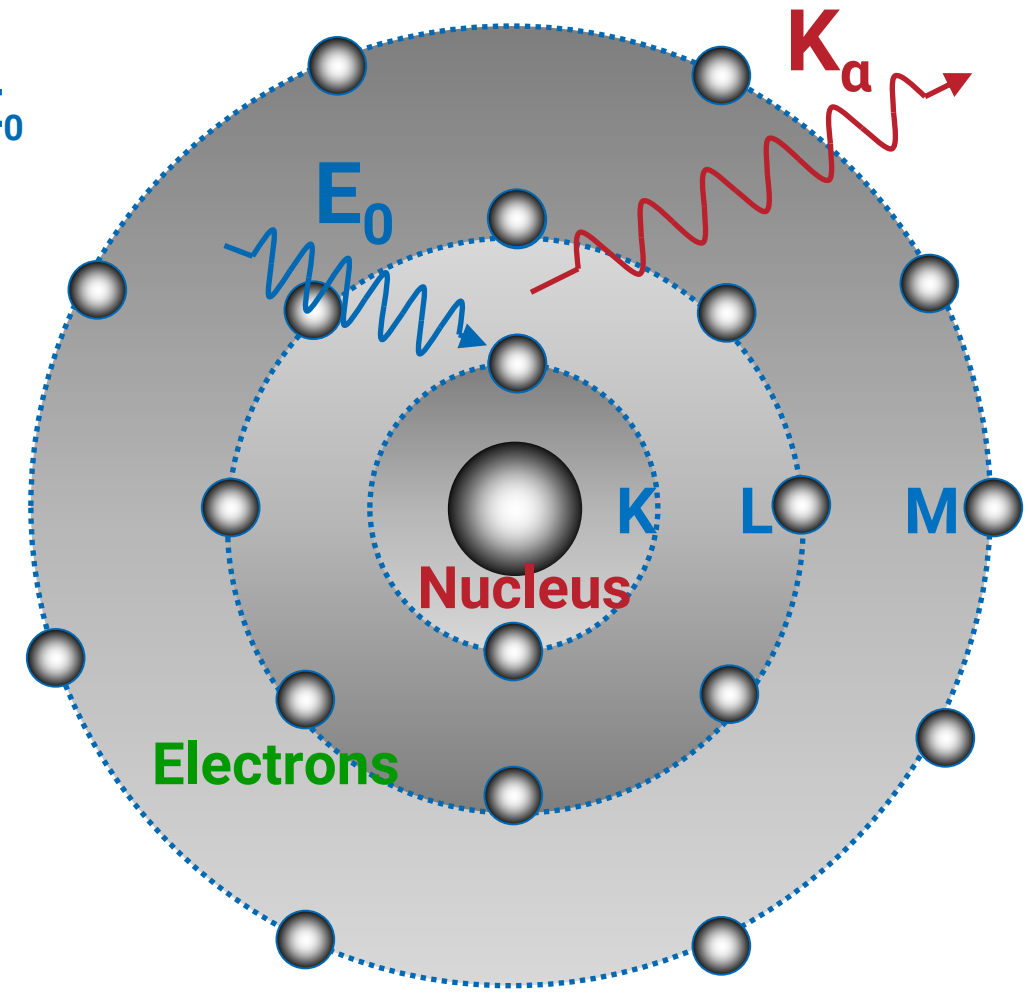


**Photo-Ionization of atomic bound electrons** (K, L, M) (**Photoelectric absorption**)

Fluorescence X-ray emission is **isotropic**

Electronic transition and emission of element
→ **characteristic fluorescence** radiation

# De-excitation: Fluorescence/Auger

Emission of characteristic X-ray

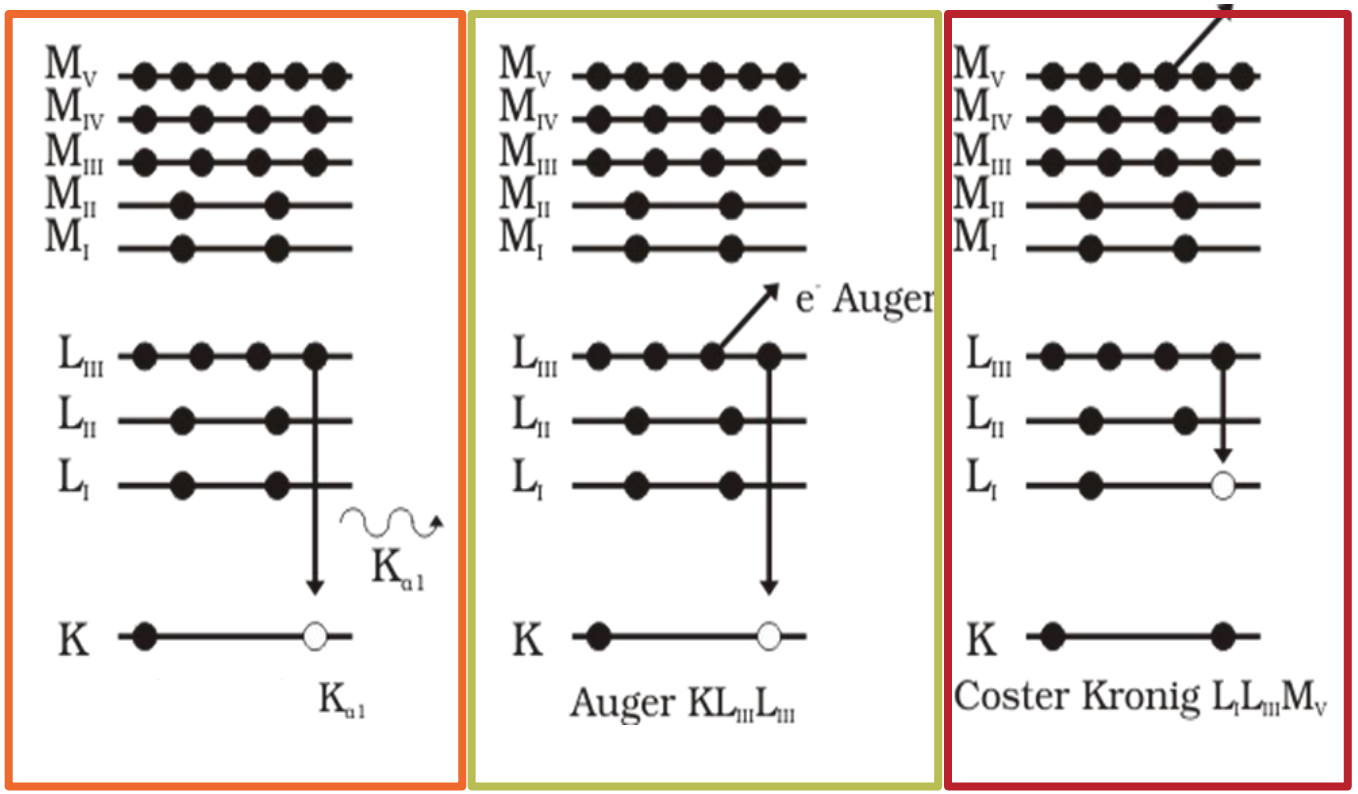


Emission of electron (vacancy filled by electron from the same shell)

Emission of electron (vacancy filled by electron from different shell)

# Fluorescence yield

The fluorescence yield is given by the **ratio of the emitted fluorescence photons over the number of the created holes**. The competing process is the **emission of Auger electrons** as the atom returns to its ground state

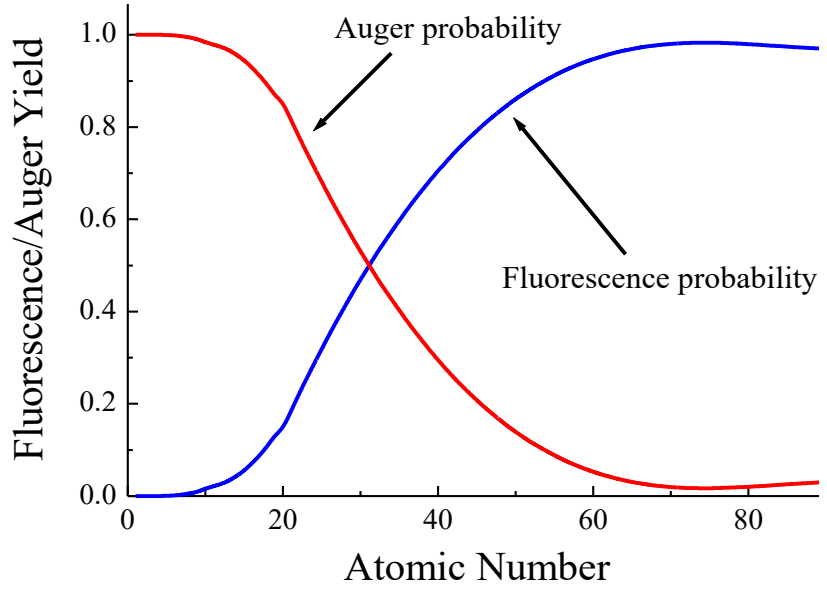


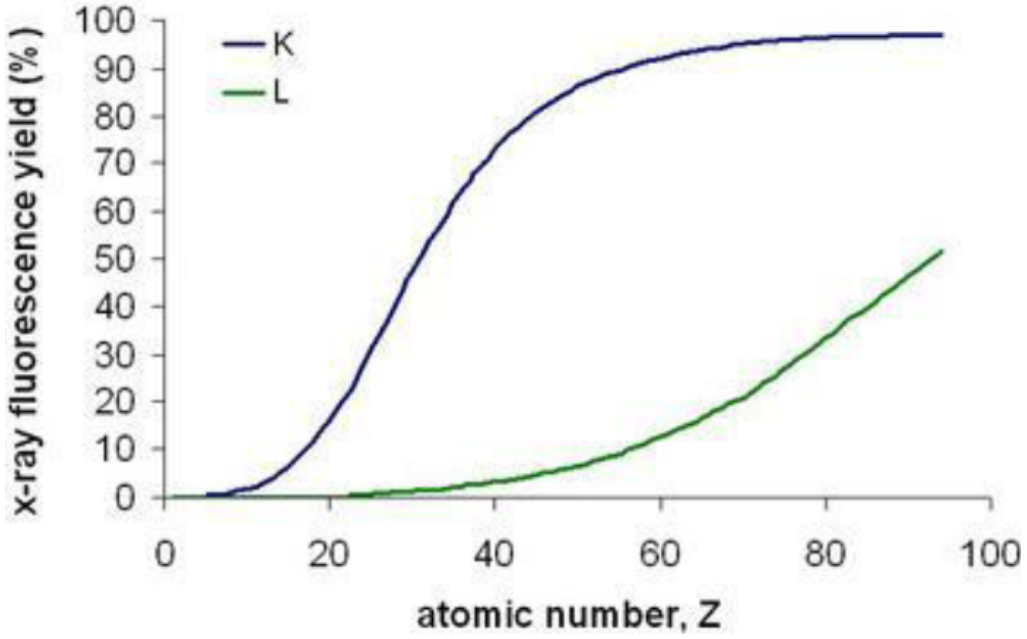


**For low-Z elements the Auger electron emission is dominant**

# Emission of characteristic X-rays

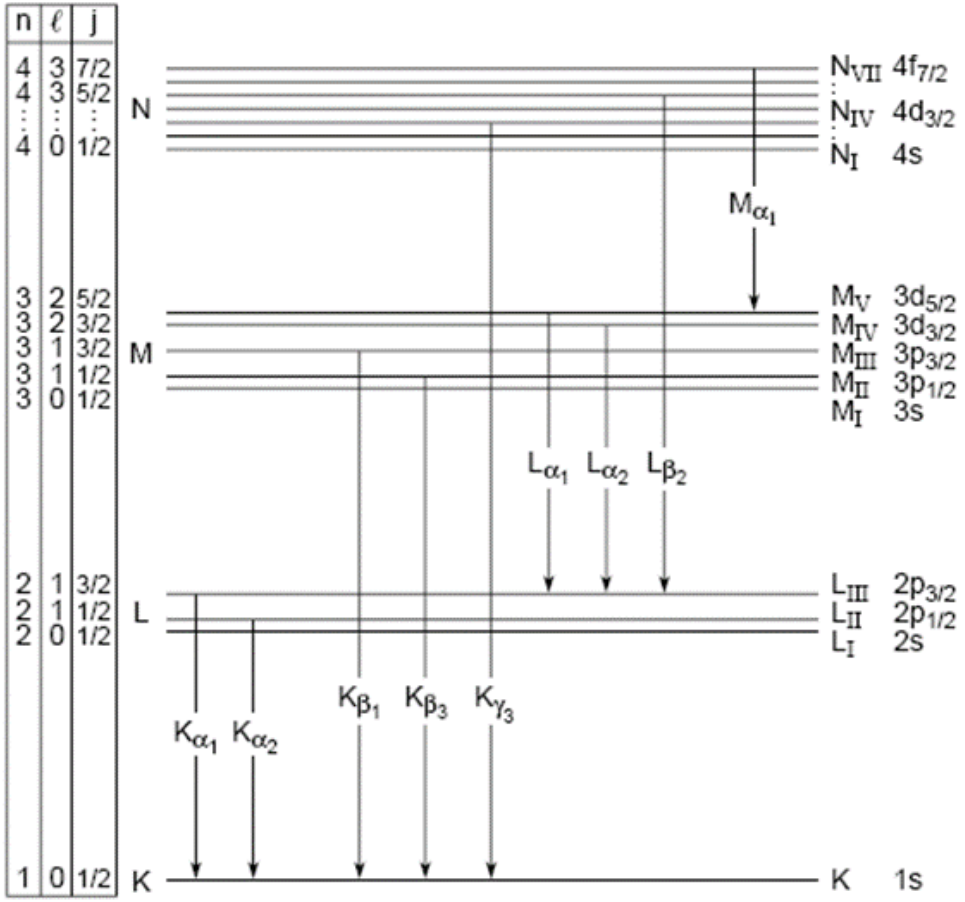


The emission of characteristic X-ray lines follows allowed electronic transitions between specific subshells

Each element has a unique set of emission lines

**Siegbahn/IUPAC notation:**

**$K_\alpha$**: $K\text{-}L_2 + K\text{-}L_3$

**$K_\beta$**: $K\text{-}M_2 + K\text{-}M_3$

**$L_\alpha$**: $L_3\text{-}M_4 + L_3\text{-}M_5$

**$L_{\beta 1}$**: $L_2\text{-}M_4$

**$L_{\beta 2}$**: $L_3\text{-}N_5$

# X-ray energies

## Moseley's law

$$E = h \cdot A \cdot R \cdot (Z - b)^2$$

*h* = Planck constant
*R* = Rydberg frequency
*Z* = atomic number
*A* = 3/4 for $K_\alpha$, 5/36 for $L_\alpha$
*b* = 1 for $K_\alpha$, 7.4 for $L_\alpha$

| | | |
|---|---|---|
| **$K_\alpha$** | $E$ [eV] ≈ 10.20 · $(Z - 1)^2$ | $E_{Fe\text{-}K\alpha}$ ≈ 6380 eV |
| **$L_\alpha$** | $E$ [eV] ≈ 1.89 · $(Z - 7.4)^2$ | $E_{Pb\text{-}L\alpha}$ ≈ 10520 eV |

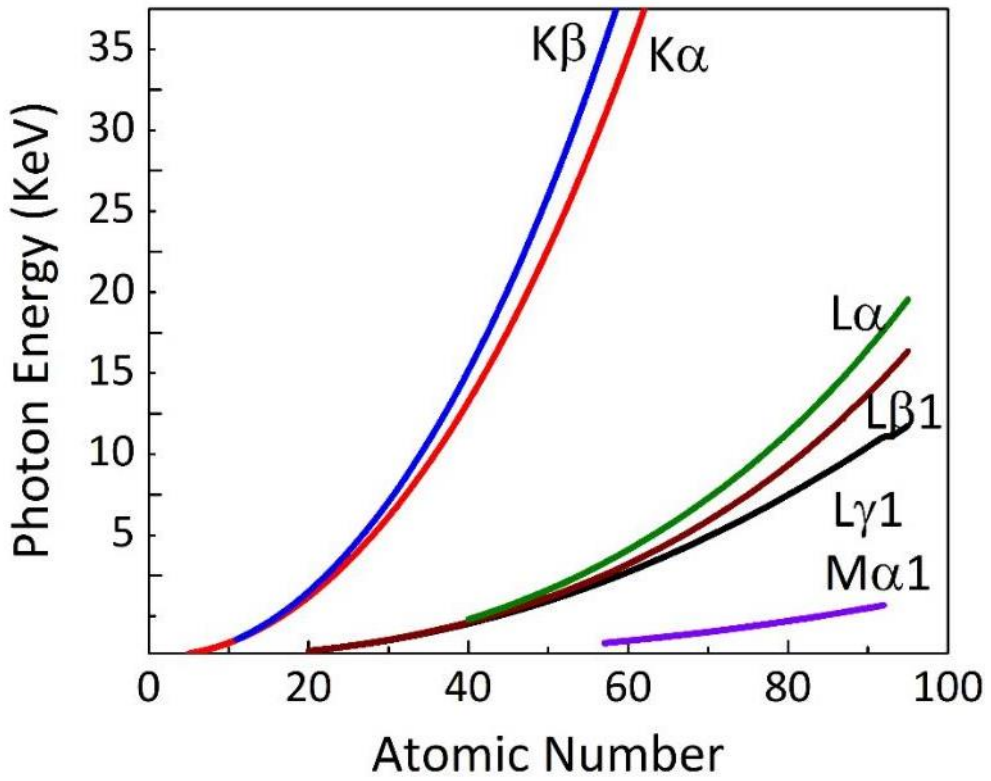


X-ray spectroscopy within the energy range 1÷30 keV offers in principle the possibility to detect all the periodic table elements ($Z$ > 10) through their K, L or even M series of emission lines

# X-ray scattering

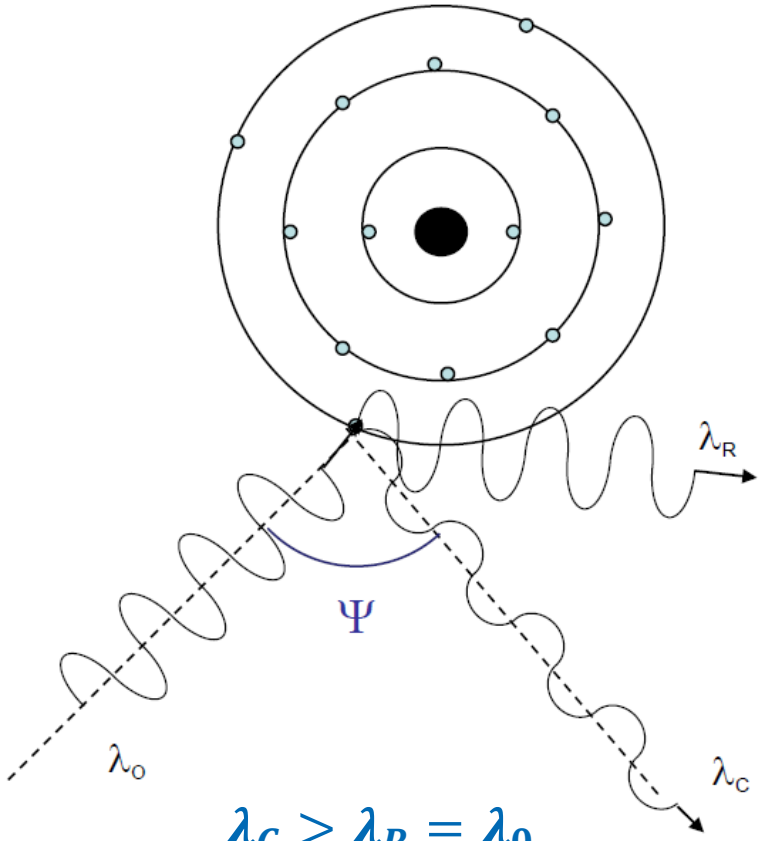


$$\lambda_C > \lambda_R = \lambda_0$$

$$\lambda_C - \lambda_0 = \frac{h}{m_e c}(1 - \cos\vartheta)$$

**Elastic/coherent scattering (Rayleigh)**:
no energy loss after collision with electrons. The Rayleigh effect is present when electrons are strongly bound.
Rayleigh is more intense for high *Z* (= heavy) matrices

**Inelastic/Incoherent scattering (Compton)**: energy loss after collision with electrons. The Compton effect is present when electrons are loosely bound.
Compton is more intense for low *Z* (= light) matrices

Both kind of scattering are **anisotropic** (the set-up geometry can be chosen to minimize the contribution of the scattering in the spectrum)

# Linear attenuation coefficient μ

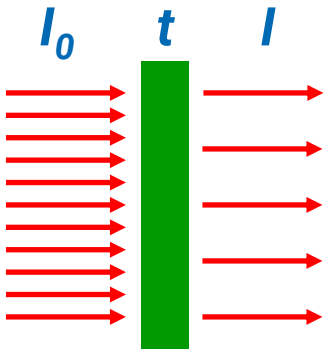


Attenuation of photons by a thin layer of thickness *dt* is described by

$$dI = I \cdot \mu \cdot dt$$

where *I* is the number of photons per unit area and unit time (photon flux) of which *dI* are attenuated while penetrating the layer of a material characterized by the (**total, linear**) **attenuation coefficient *μ***. This is equivalent to

$$I = I_0 \cdot e^{-\mu \cdot t}$$

*I* and $I_0$ are the photon fluxes behind and in front of the absorber, respectively, and *t* is the thickness. *μ* is a function not only of the material (atomic number *Z*) but also of the photon energy *E*

# Mass attenuation coefficient $\mu_m$

$$\mu = \mu_m \cdot \rho$$

the total mass attenuation coefficient $\mu_m$ doesn't depend on the density $\rho$ of the material.

The coefficient $\mu_m$ summarizes all possible photon interactions

$$\mu_m = \tau_m + \sigma_m$$

where $\tau_m$ describes the photo absorption and $\sigma_m = \sigma_{coh} + \sigma_{inc}$ are the contributions by coherent and incoherent scattering, respectively.

Both kinds of scattering contribute much less than the photo absorption to the total $\mu_m$

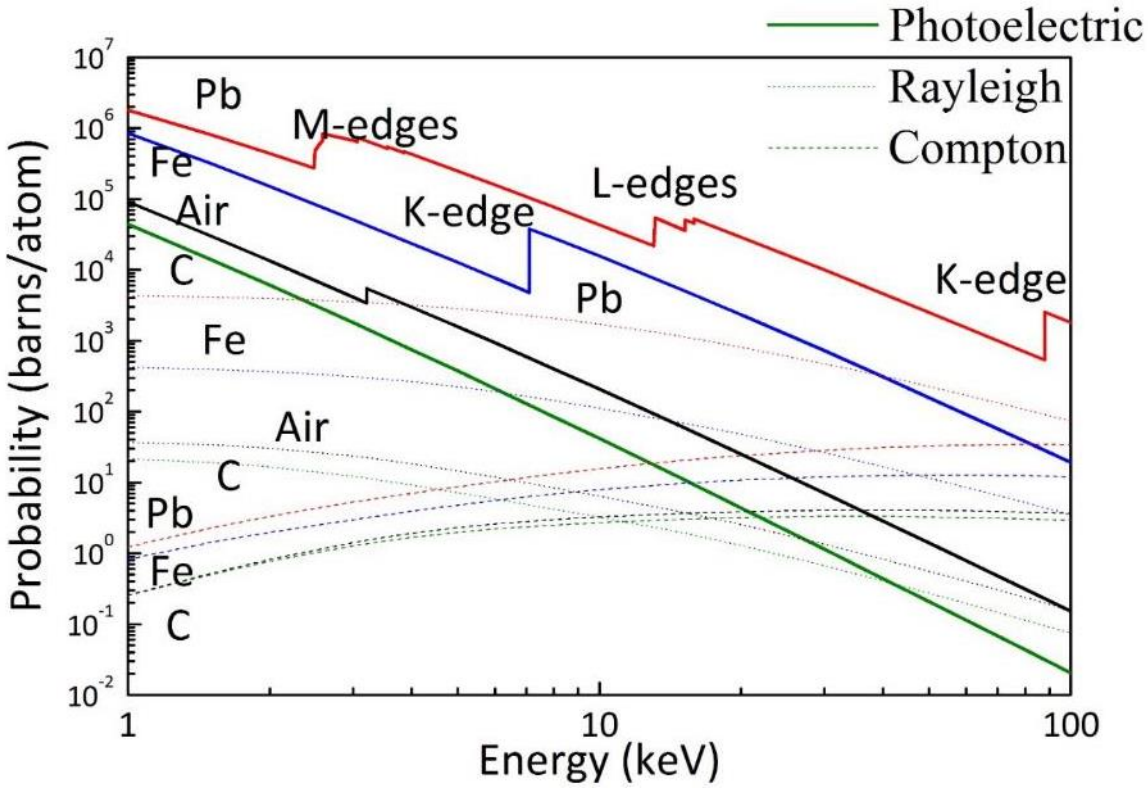


area-related mass $m = M/A$ (mass $M$ per unit area $A$), $t \cdot \rho = M/A$, in grams/cm$^2$

# Detectors for XRF

- Proportional Counters
- Scintillation Detectors
- Si(Li)
- LEGe
- PIN Diode
- **SDD**
- CCD, CMOS cameras
- CZT, other

Wavelength dispersive XRF (WDXRF)

Energy dispersive XRF (EDXRF)

# Efficiencies of different detectors

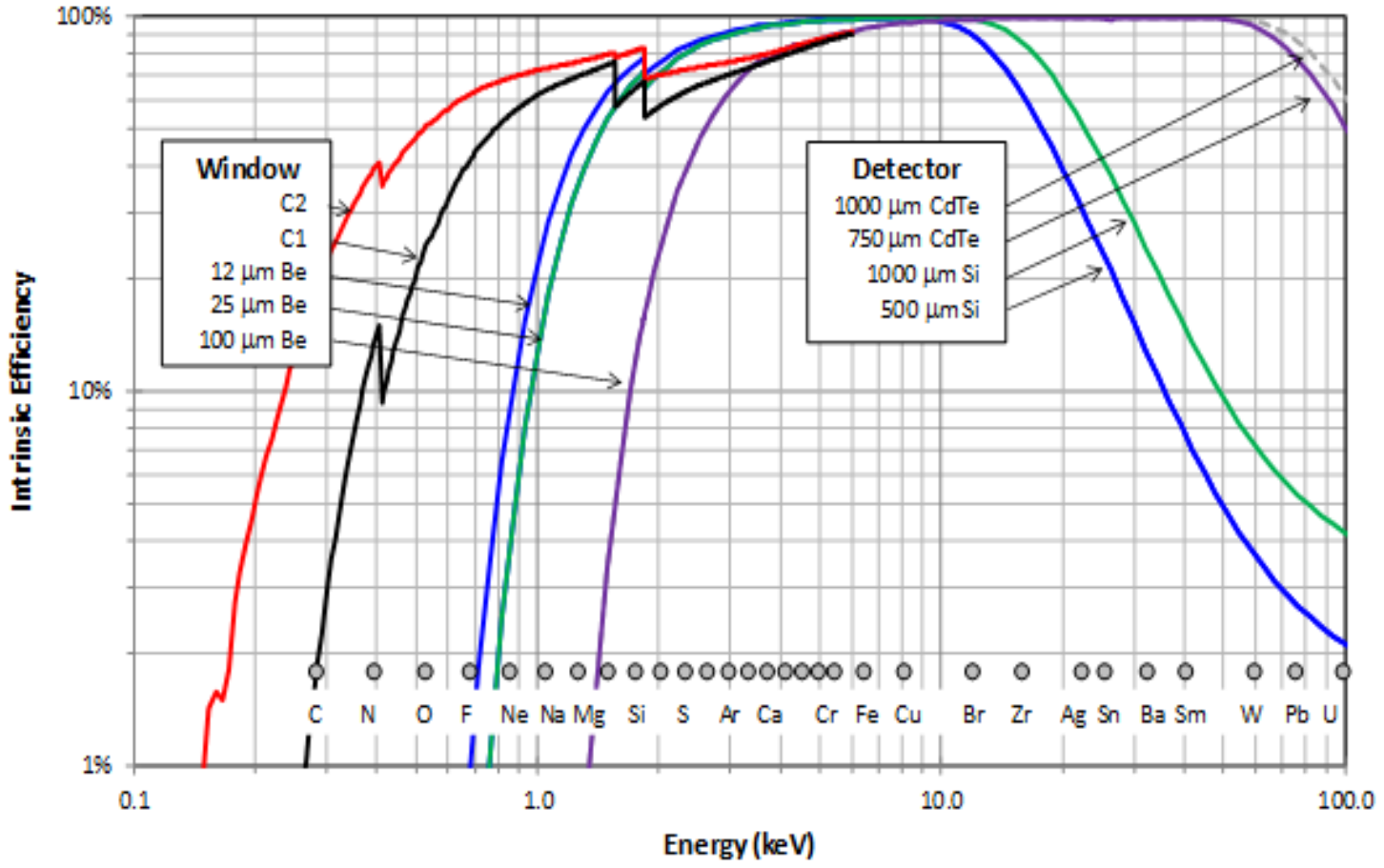


Comparison of different detector's efficiency from AMPTEK
https://www.amptek.com/products/x-ray-detectors/fastsdd-x-ray-detectorsfor-xrf-eds/fastsdd-silicon-drift-detector

# “Light” elements (Na, Mg, Al, Si)

**Vacuum** atmosphere or **He flushing** is required in the x-rays path between sample and detector

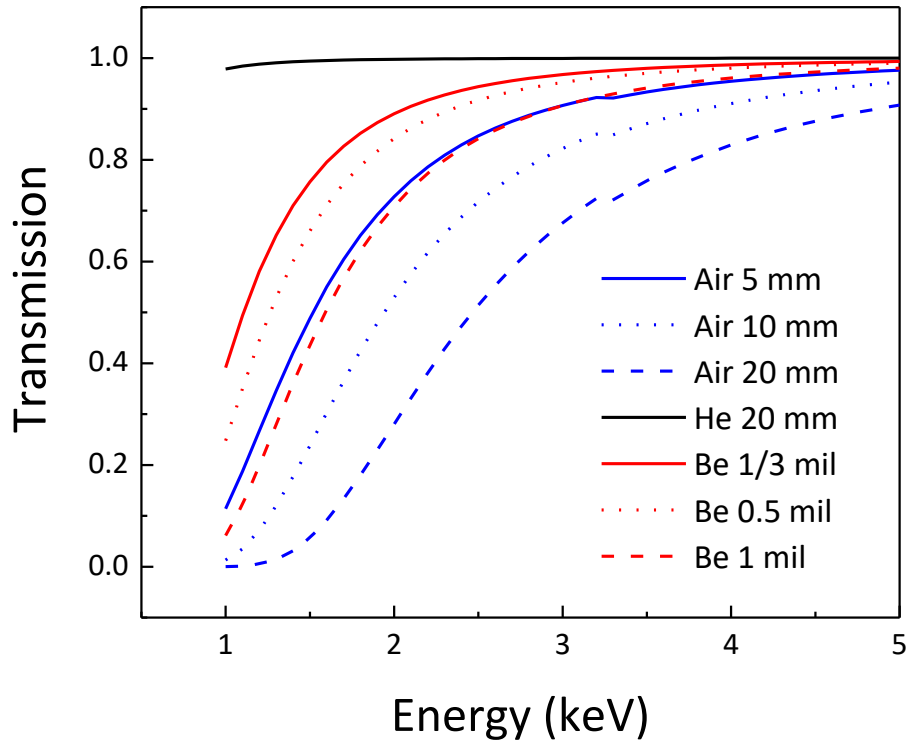


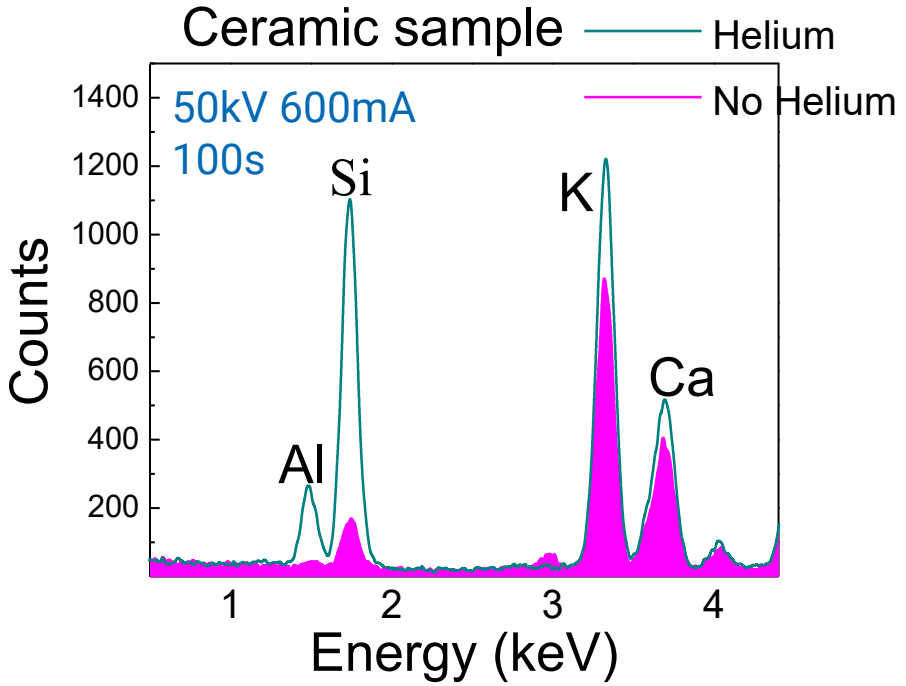


The improvement in the intensity of Al-K and Si-K characteristic X-ray lines is significant, about 22 and 7.3 times respectively

# Typical EDXRF spectrum

- Escape peaks (Ca-Ka – 1.74 keV = 1.95 keV)

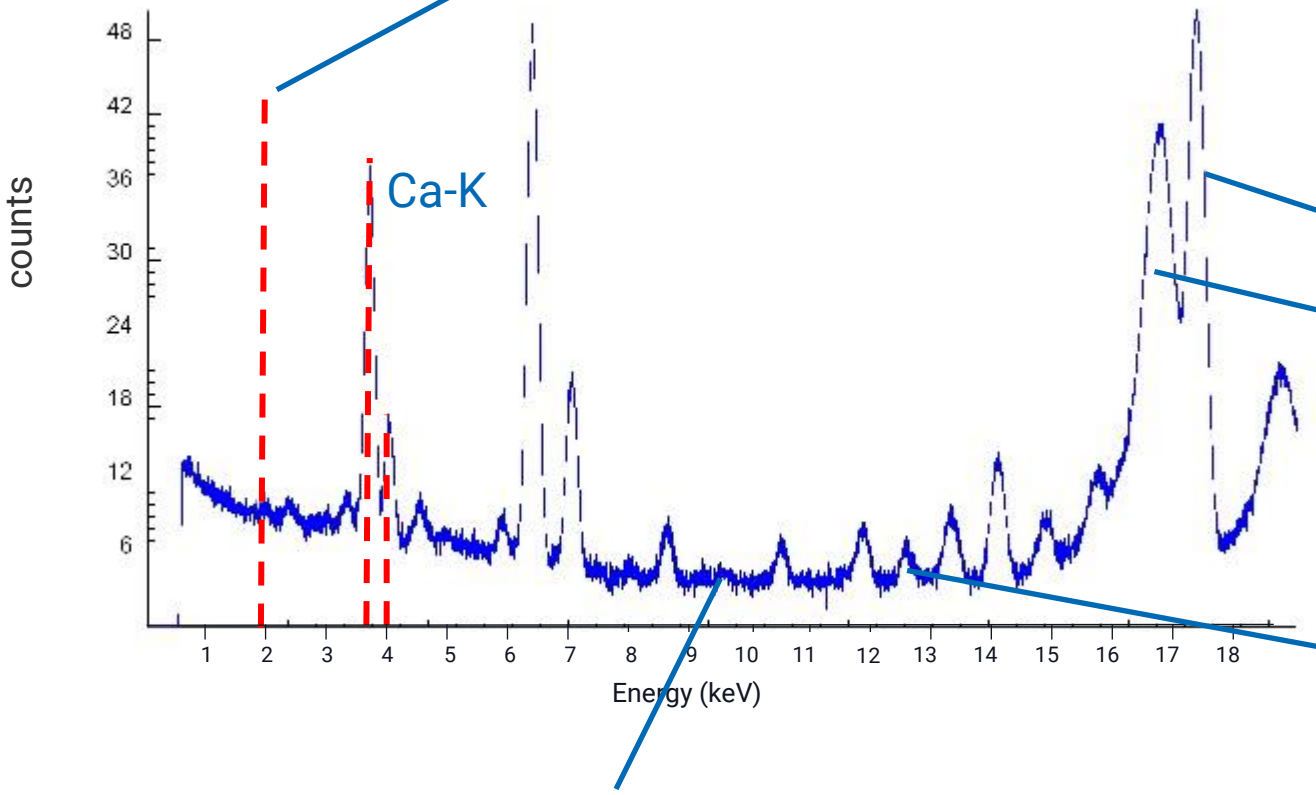


- Characteristic radiation
  - ✓K, L or M-lines
- Scatter
  - ✓Coherent
  - ✓Incoherent
- Sum peak

  Fe-Ka + Fe-Ka= 12.8 keV
- Continuum radiation

# Resolution of EDXRF spectrometers

Full Width at Half Maximum (FWHM) of a peak

$$FWHM_{Peak}^2 = FWHM_{Elec}^2 + FWHM_{Det}^2$$

Electronic noise:
~100 eV

Intrinsic contribution:

$$2.3548\sqrt{\varepsilon \times F \times E}$$

$\varepsilon$ Energy to create e-h pair (3.85 eV)

$F$ Fano factor (~0.114)

$E$ X-ray energy in eV

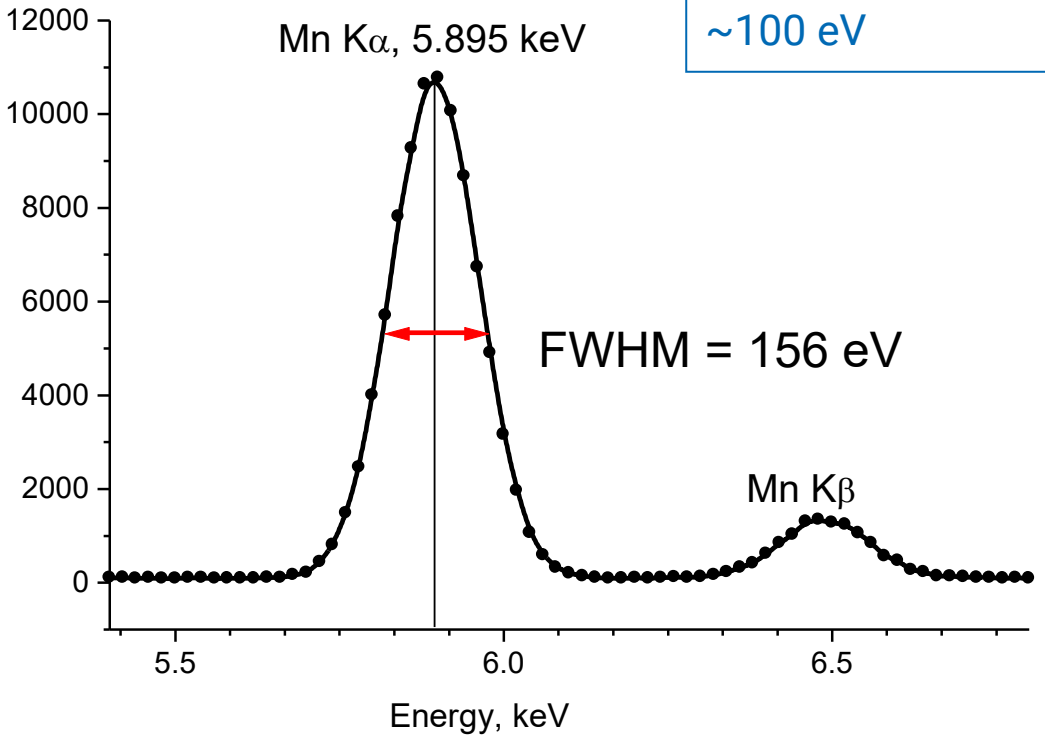


Mn Kα @ 5.895 keV

$FWHM_{Det}$ = 120 eV

$FWHM_{Elec}$ = 100 eV

=> $FWHM_{Peak}$ = 156 eV

# Overlaps of peaks, fitting

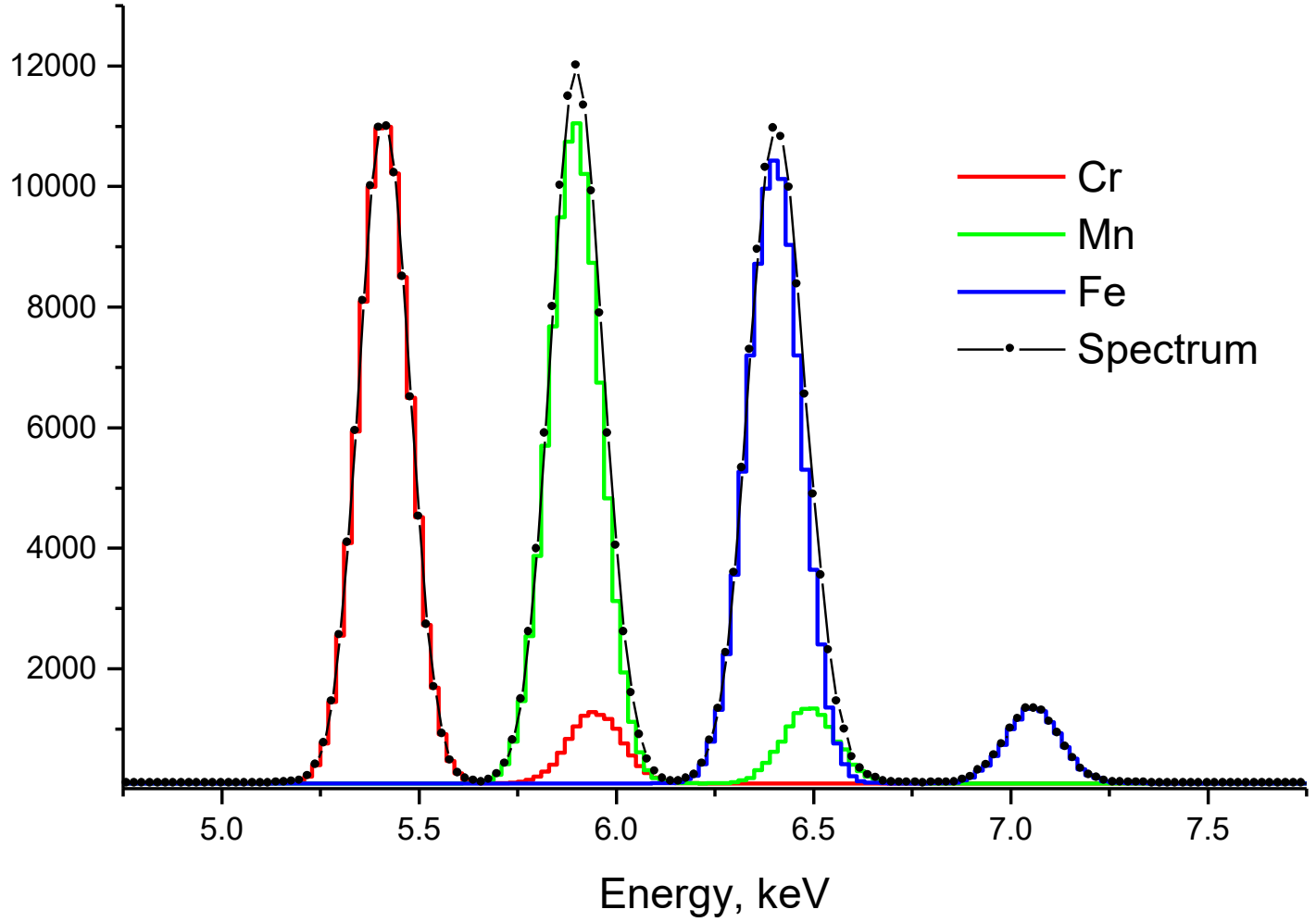


Detector resolution ~160 eV

Resolution of modern SDDs can be around 130 eV

# Case of strong overlapping

Overlapping of As-Kα (about 10.54 keV) and Pb-Lα lines (about 10.55 keV)

**Binding energies:**

**As-K = 11.87keV**
**Pb-$L_3$ = 13.04keV**
**Pb-$L_2$ = 15.20keV**
**Pb-$L_1$ = 15.86keV**

X-ray energies (ST)
Mo-Kα = 17.48keV
Zr-Kα = 15.78keV
Br-Kα = 11.92keV

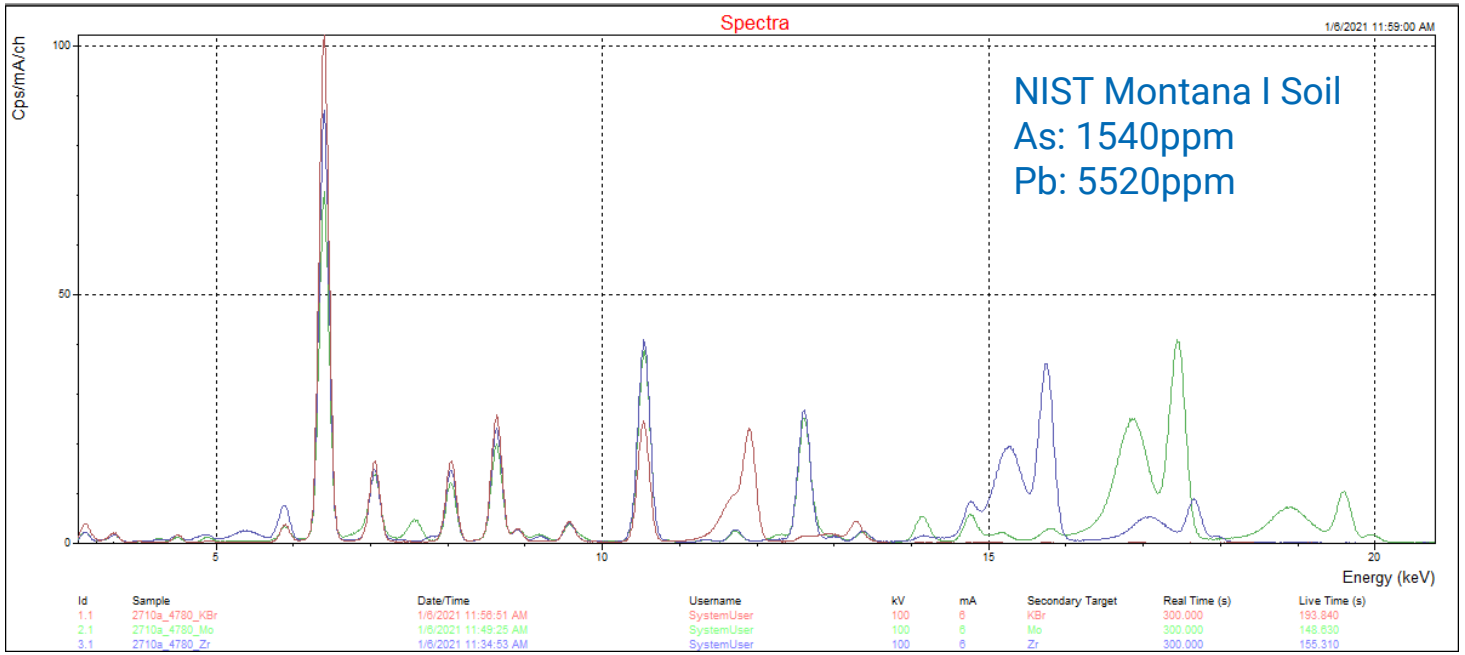


obtained with a secondary target ED-XRF spectrometer using 3 different targets

**This problem can be overcome with synchrotron light, as arsenic can be easily quantified using an energy ranging between 11.87 keV and 13.04 keV**

# Comparison of overlapping lines

| Lines overlapping | Difference | Good aspect | Bad aspect |
|---|---|---|---|
| As $K_\alpha$: 10544 eV<br>Pb $L_\alpha$: 10552 eV | ~ 8 eV | • Element generally in similar level of concentration<br>• Possibility of using secondary lines<br>• Possibility of exciting separately the lines of one element (monochromatic radiation) | Extremely strong overlapping |
| Fe $K_\beta$: 7058 eV<br>Co $K_\alpha$: 6930 eV | ~ 128 eV | Weak overlapping | In environmental samples, Fe concentration is orders of magnitude higher than Co one |

# The Sherman-Nikina formula

$$N_i = \varepsilon(E_i) w_i \int_{E>E_i^{ab}}^{E_{\max}} G\ K_i\ A(E, E_i)\ R_i\left(E, E_j\right) N(E)\ dE$$

$$A_s(E, E_i) = \frac{1 - e^{-\left[\frac{\mu_s(E)}{\sin\theta_1} + \frac{\mu_s(E_i)}{\sin\theta_2}\right]\rho X}}{\frac{\mu_s(E)}{\sin\theta_1} + \frac{\mu_s(E_i)}{\sin\theta_2}}$$

Attenuation in the sample

$$K_i(E) = \frac{J_i^k - 1}{J_i^k} w_i^k f_i^{K\alpha} \tau_i(E)$$

X-ray production (all FP)

$R_i\left(E, E_j\right)$ Enhancement of x-ray production of element *i* by elements *j*

$N(E)$ Is the distributioon by energies of the excitation radiation

$\varepsilon(E_i)$ Is the efficiency of the detector for energy $E_i$

$G$ Is the overall effective solid angle

At synchrotron, the primary radiation is monochromatic ($E_0$):

$$N_i = \varepsilon(E_i) w_i\ G\ K_i\ A(E_0, E_i)\ R_i\left(E_0, E_j\right) N(E_0)$$

# Sensitivity

Quoting of the change in an **indication** of a **measuring system** and the corresponding change in a **value** of a **quantity** being measured

Response of the instrument to the **unit of concentration** (or **areal density**) of a given element

$$N_i = \varepsilon(E_i) w_i \; G \; K_i \; A(E_0, E_i) \; R_i\left(E_0, E_j\right) N(E_0)$$

$$N(E_0) = I(E_0) \; t_{meas}$$

If $I(E_0)$ is constant: $S_i(E_0) = \frac{N_i}{w_i \; t_{meas}} = \varepsilon(E_i) \; G \; K_i \; A(E_0, E_i) \; R_i\left(E_0, E_j\right) I_0(E_0)$

If $I(E_0)$ is not constant: $S_i(E_0) = \frac{N_i}{w_i \; t_{meas} \; I(E_0)} = \varepsilon(E_i) \; G \; K_i \; A(E_0, E_i) \; R_i\left(E_0, E_j\right)$

# Elemental sensitivities, Exp. vs MC

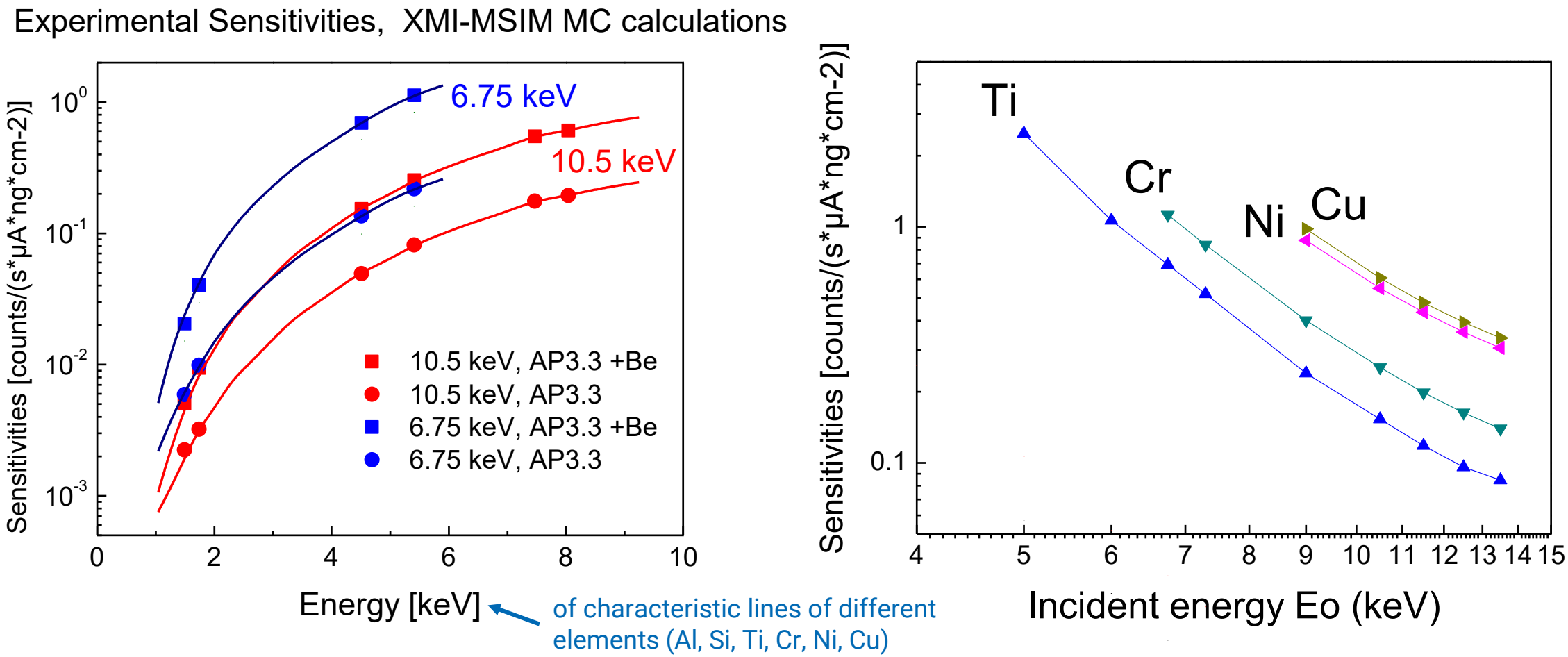


of characteristic lines of different elements (Al, Si, Ti, Cr, Ni, Cu)

Data from the XRF beamline at Elettra Sincrotrone Trieste (now dismantled)

# Detection Limits

**Spectrum = SIGNAL + NOISE**

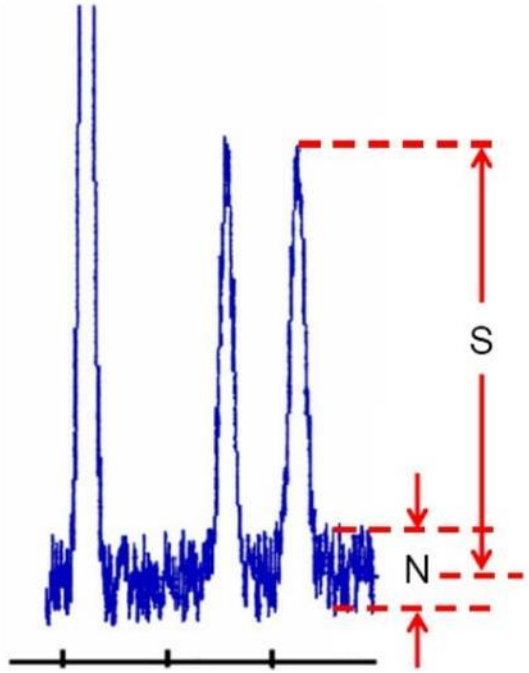


**SIGNAL** = related to the analyte concentration (deterministic part)

**NOISE** = random fluctuation (stochastic part)

If the signal to noise ratio (S/N) is too low, we cannot distinguish the signal from the noise fluctuations and thus not be sure that the analyte is present and determine any analyte concentration.

What is too low? How do we determine the magnitude of the noise fluctuation?

IUPAC

> limit of detection, expressed as the concentration $x_L$, is derived from the smallest measure $y_L$ that can be detected with reasonable certainty

# Detection Limits in XRF analysis

The blank signal $N_{bl}$ is ruled by Poisson probabilistic distribution, therefore the standard deviation of the noise signal is the square root of $N_{bl}$

$$LOD_i = \frac{3\sigma_{bl}}{S_i\, t_{meas}} = \frac{3\sqrt{N_{bl}}}{S_i\, t_{meas}} = \frac{3\sqrt{N_{bl}}}{\frac{N_i}{w_i}} = \frac{3\sqrt{N_{bl}}\, w_i}{N_i} \qquad S_i(E_0) = \frac{N_i}{w_i\, t_{meas}}$$

If $I(E_0)$ is constant

THUS: the detection limit

- increases with the square root of the background
  10x higher background ➡ 3 times higher DL
- decreases with the square of the measurement time
  counting 10x longer ➡ 3 times lower DL
- decreases linearly with the sensitivity
  10x more sensitivity ➡ 10 times lower DL

# Detection Limits in XRF analysis

**What is the blank signal $N_{bl}$?**

- Continuum counting
- Sample blank
- Instrumental background
- Spectral interference

Sample blanks:
- elements present in sample support (filters for the analysis of APM)
- elements introduced during sample preparation (fused sample) …

Background (instrumental):
- spurious peaks from fluorescence of excitation chamber
- lines from primary beam

Sample blanks and instrumental background need to be determined very accurately:
- the value of these contributions shall be subtracted from the measurement result
- and their standard deviation shall be added to the combined uncertainty

# Comparison of spectra (clay ISE 952)

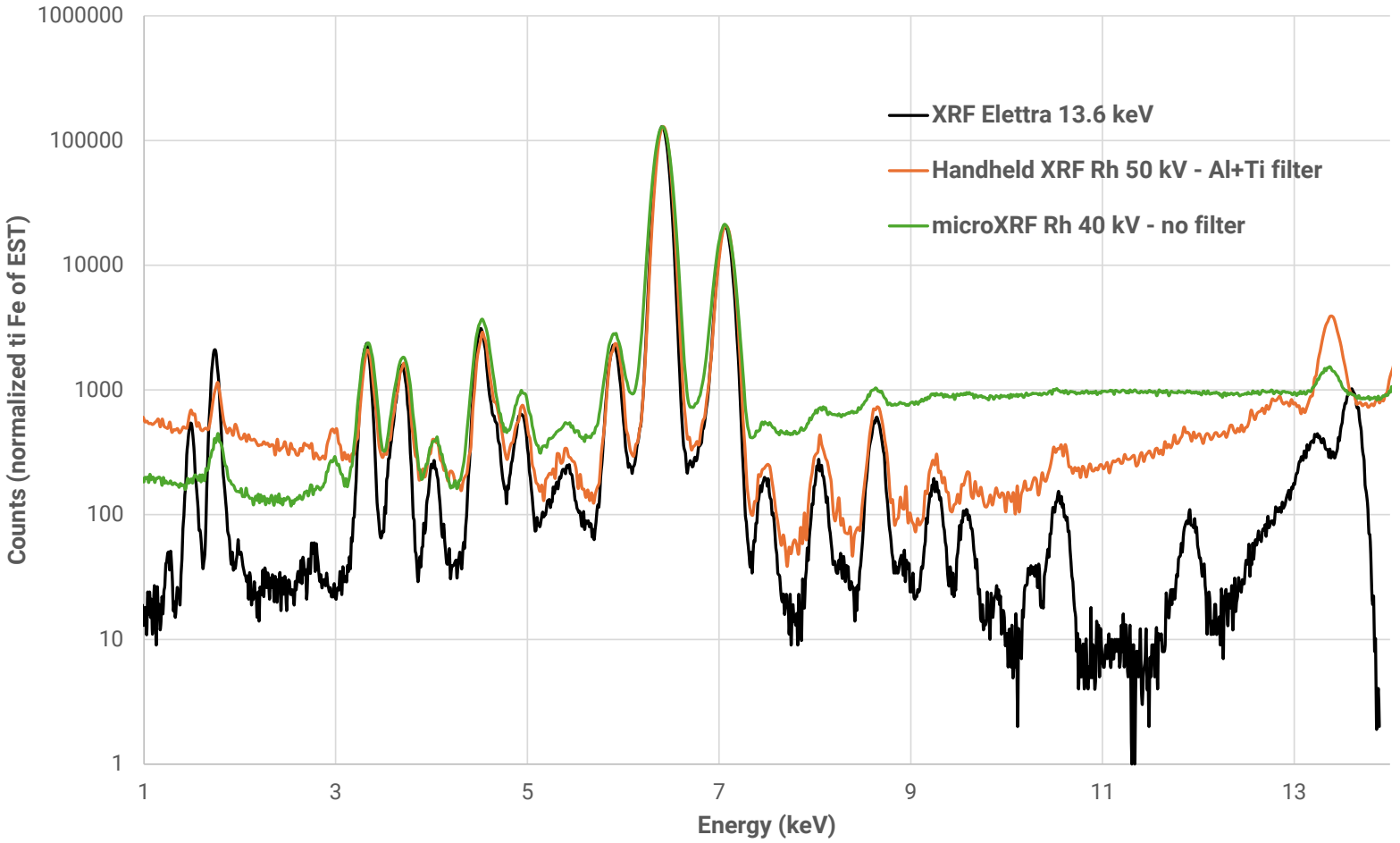


Courtesy of A.G.Karydas, (National Center for Scientific Research "Demokritos", Greece)

# SR vs Benchtop (TXRF, DLs Water)

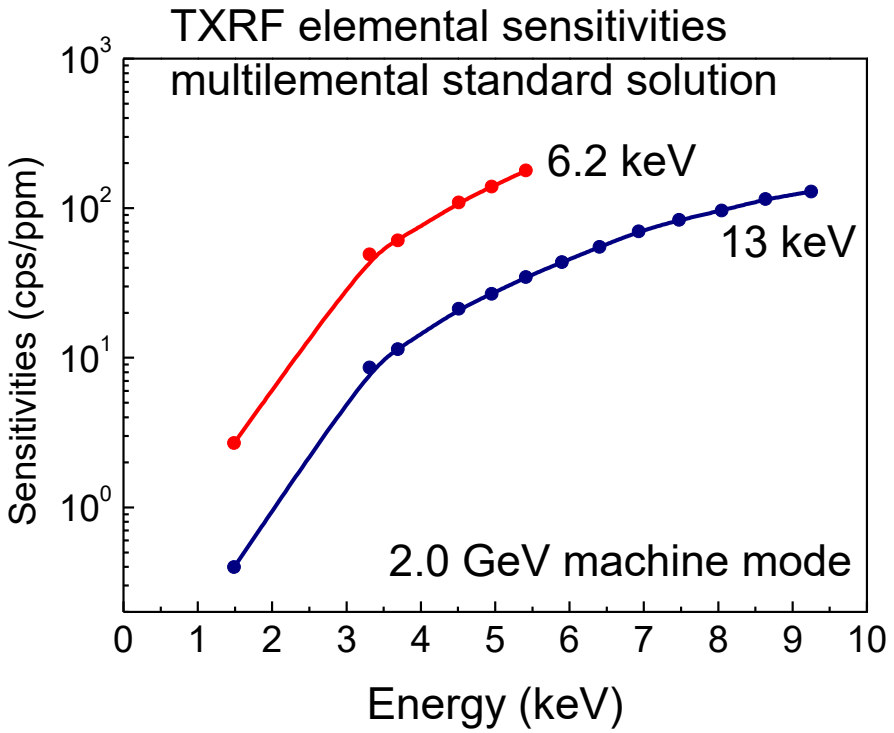


- **Factor 160** better for light elements (K, Ca) using SR-TXRF, at the range of **2-3 ppb**
- For mid elements: **30-50 times better** using SR-TXRF (LOD ~ 1 ppb wastewater, <1 ppb down to **0.2 ppb** for other water samples)
- For high Z elements Cd-Sn-Sb: **2-10 times** but for some cases benchtop is better (K-lines).

LOD (SR-TXRF) < 10 ppb

**E. Marguí[1], M. Hidalgo[1], I. Queralt[2]**
[1]Department of Chemistry, University of Girona, Girona, Spain
[2]Institute of Earth Sciences Jaume Almera ICTJA-CSIC, Barcelona, Spain

# Advantages of SL for XRF

- Higher flux
- Tunability of energy
- Polarization
- Finest achievable spatial resolution

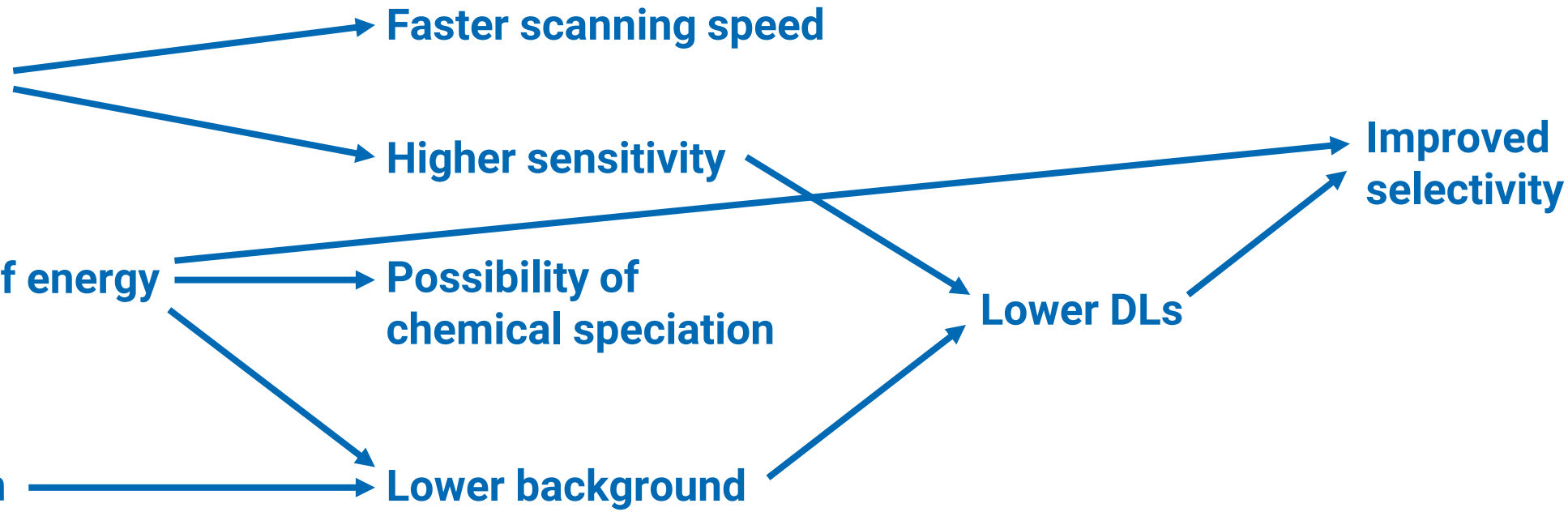

# X-ray total reflection

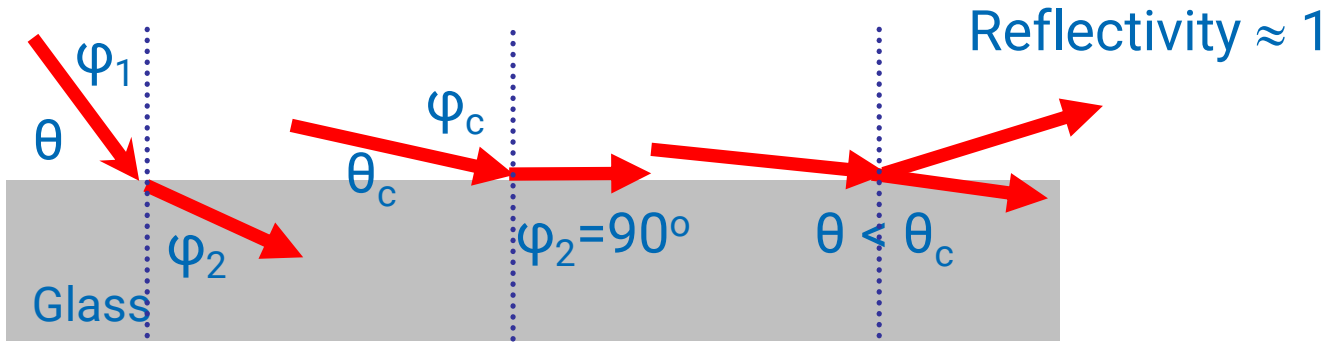


**Snell Law** $\frac{\sin\phi_2}{\sin\phi_1} = \frac{1}{n} \quad \Rightarrow \quad \sin\phi_2 = \frac{\sin\phi_1}{n} \quad \Rightarrow \quad \phi_2 > \phi_1 \quad n \approx 1 - \delta$

$\vartheta_{crit} = \sqrt{2\delta}$ $\quad \vartheta_{crit}(deg) \approx \frac{1.651}{E(keV)}\sqrt{\frac{Z}{A}\rho(\frac{g}{cm^3})}$

*Z*: Atomic number
*A*: Atomic mass
*ρ*: Density

# X-ray Standing Wave

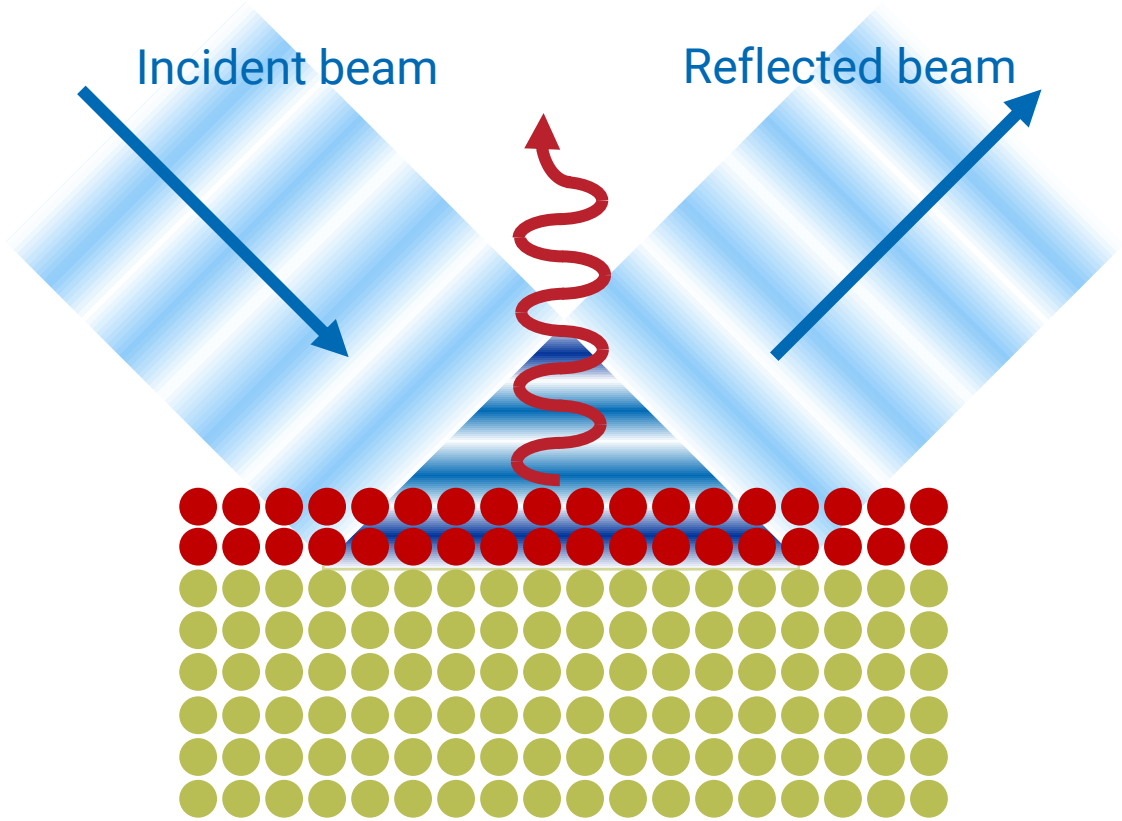


**Formation of X-ray Standing Wave (XSW) at grazing incident/exit angle**

**Electric Field Modulations above the surface**

The X-ray fluorescence intensity from the sample depends on the varying field intensity of the XSW field within the sample

# GIXRF and XRR

By varying continuously the grazing incident angle through and few times above the critical angle for TR, the recorded XRF intensity profiles (Grazing Incidence-XRF analysis) have the potential to provide information on structural and compositional properties of thin films, such as the layer composition, sequence, thicknesses and densities, interface roughness, in depth elemental gradients of matrix elements or dopants in semiconductors, characterization of nano-particles deposited on flat surfaces, etc

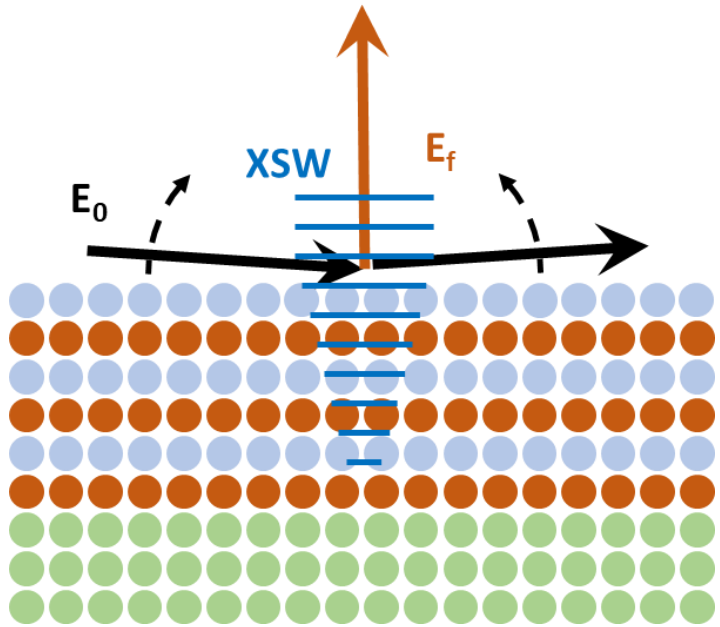


A more accurate and robust reconstruction of these thin film properties requires the synergy or even the simultaneous fitting of GI-XRF with X-ray reflectometry (XRR) data

# Total reflection X-ray Fluorescence

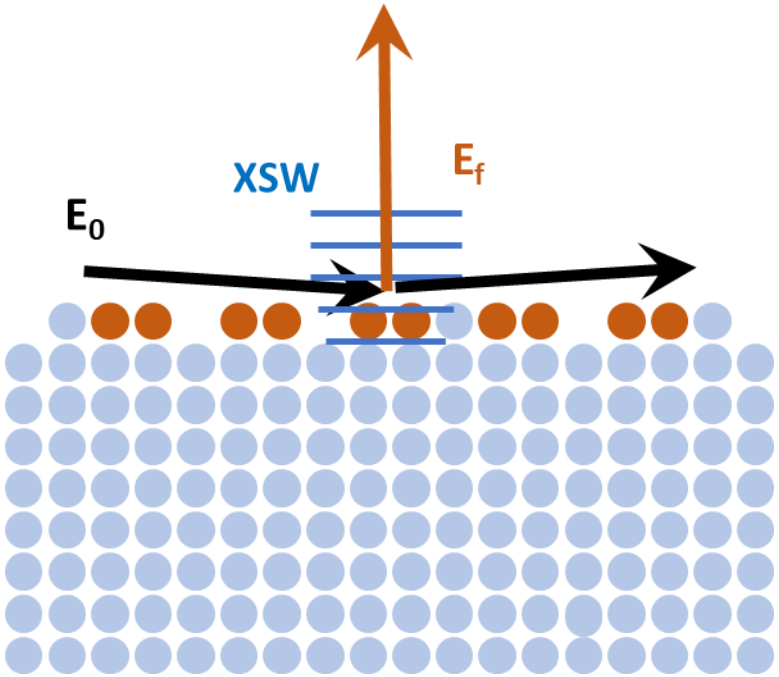


TXRF is essentially an energy dispersive XRF technique arranged in a special geometry.

Due to this configuration, the measured spectral background in TXRF is less than in conventional XRF. This reduction results in increased signal to noise ratio.

TXRF is a surface elemental analysis technique often used for the ultra-trace analysis of particles, residues, and impurities on smooth surfaces.

# Conventional XRF

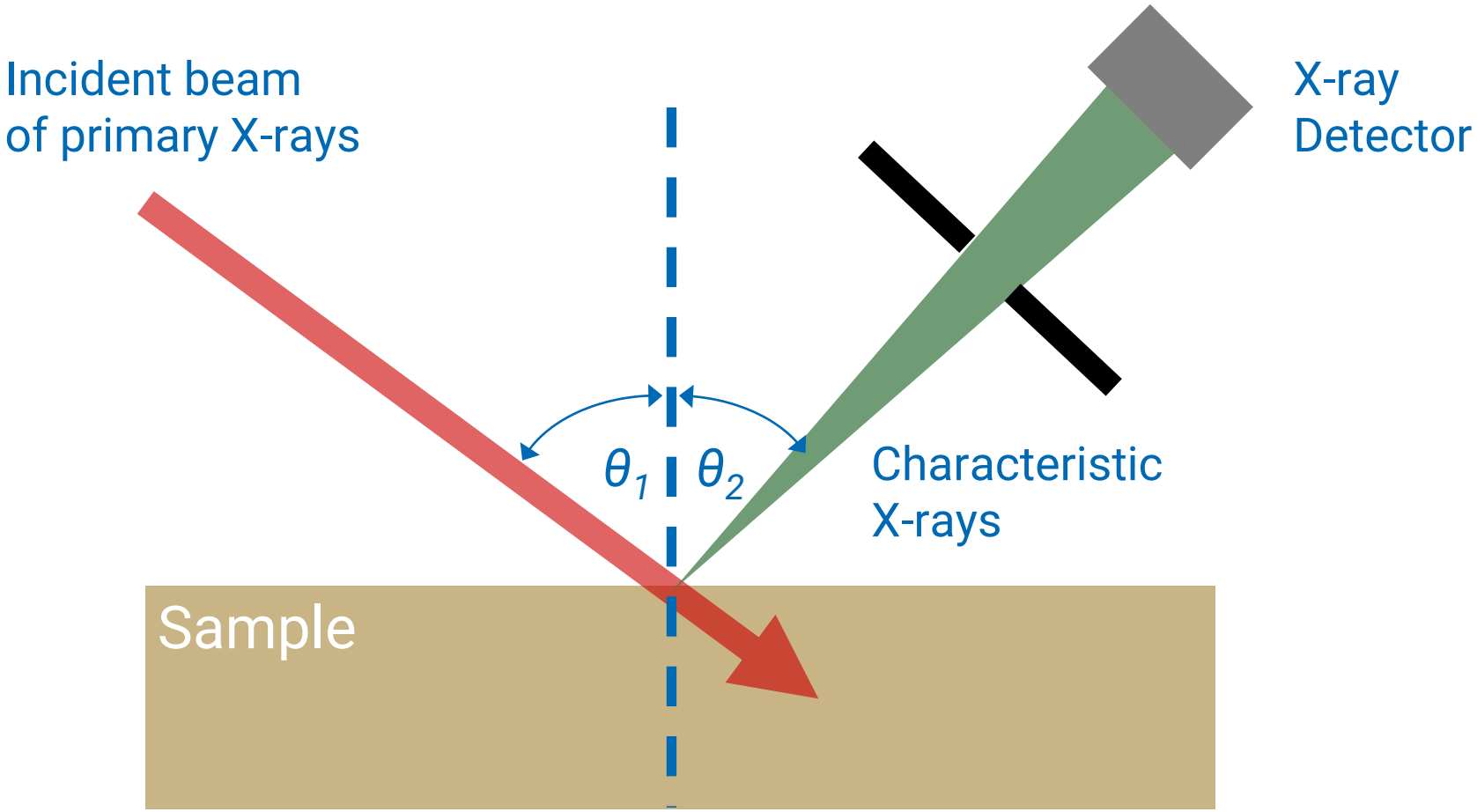

# Penetration and information depth

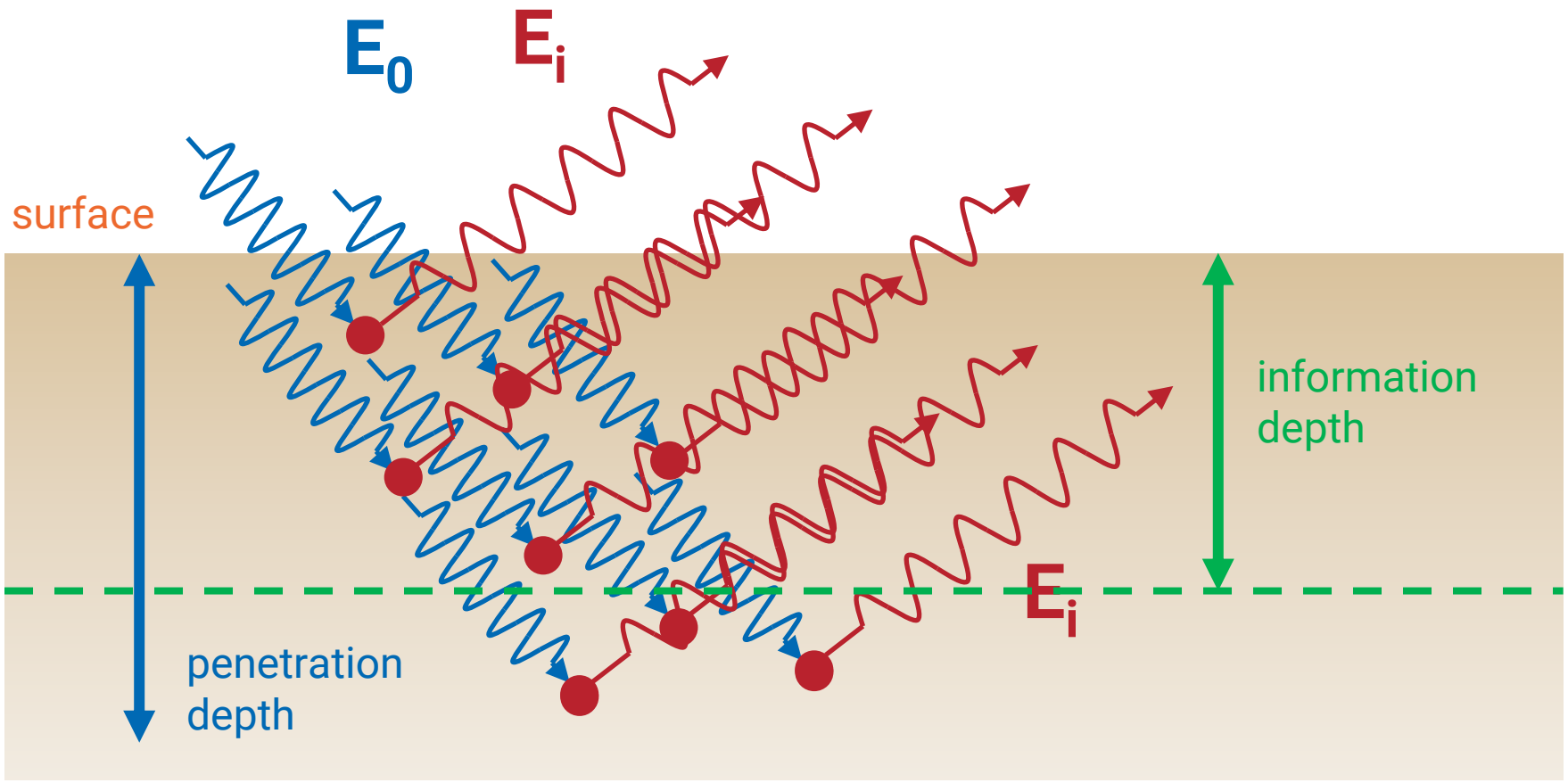

# Penetration and information depth

**Penetration and information (analytical) depth depend on the energy of the X-ray and on the matrix:**

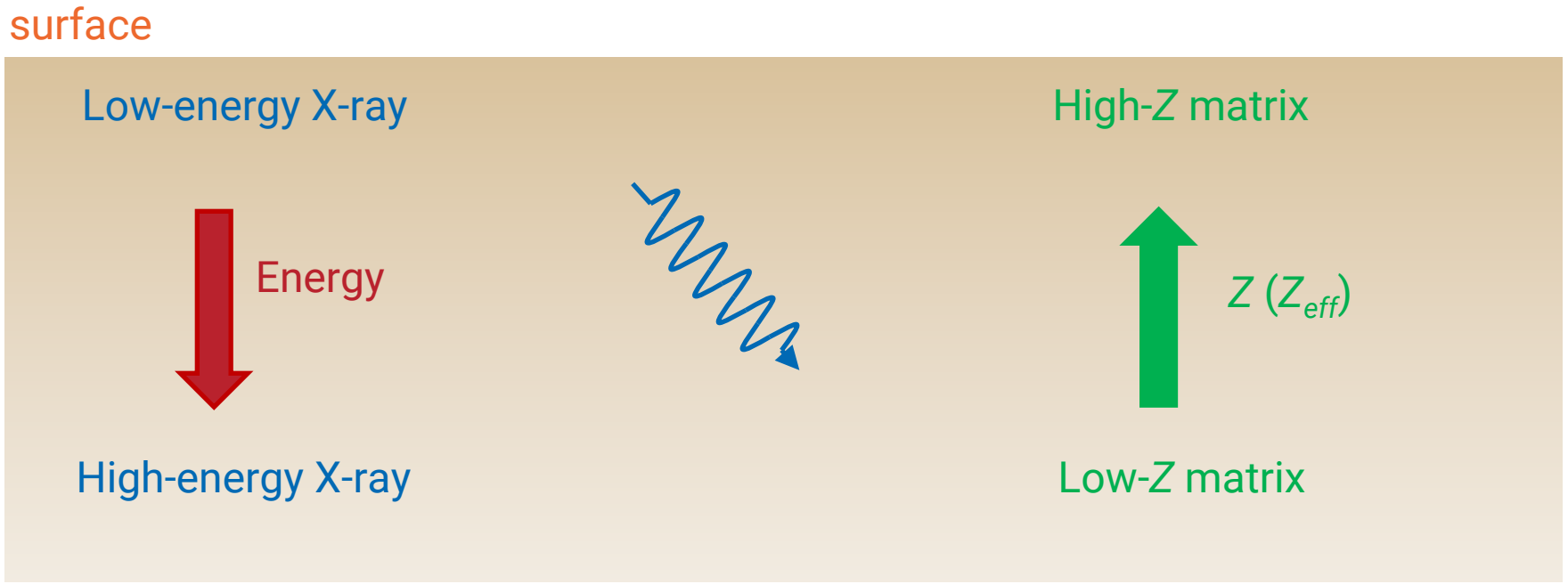


- Surface treatment is extremely important for heavy matrices
- Information thickness is essential for light matrices

# Influence of sample thickness

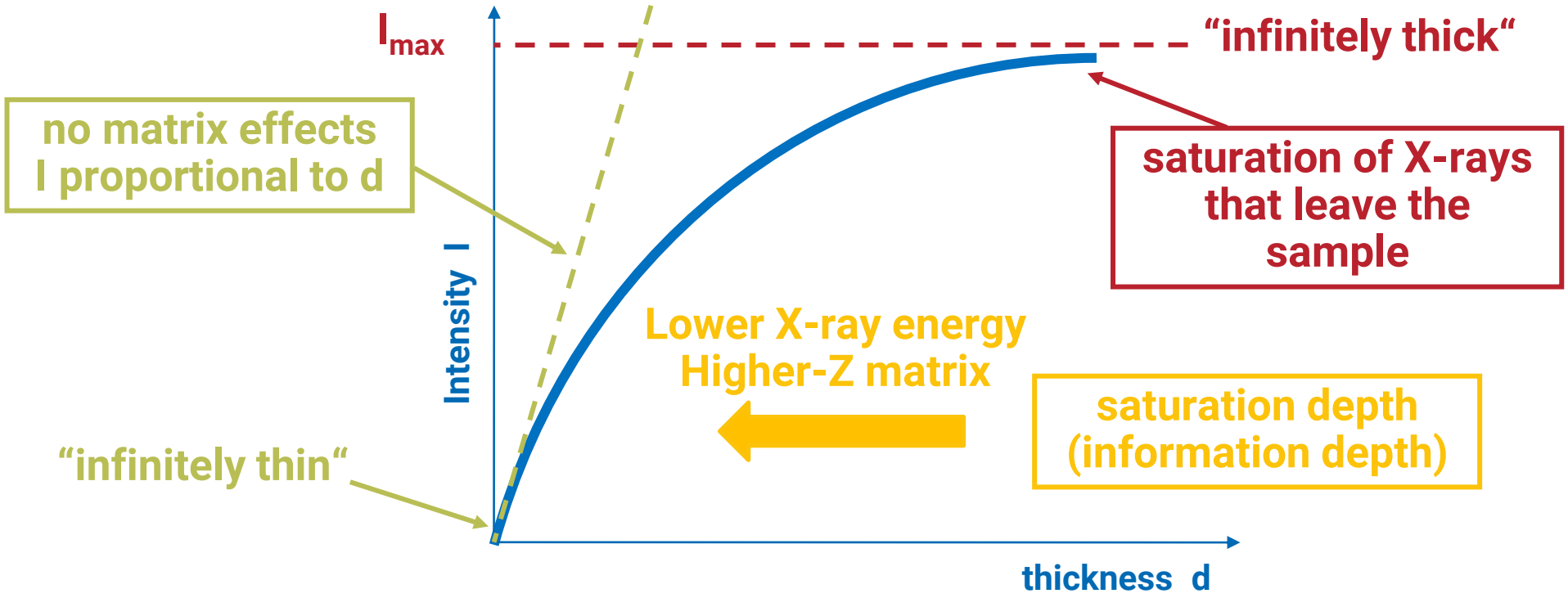


Increasing the thickness of the sample above the information depth will not increase the signal but only the scattering of the primary radiation

# Analytical depths in different matrices

**Different elements exhibit different Information thicknesses (99%), depending on their characteristic X-ray energy and on the overall matrix**

| Line | Energy | Graphite | Glass | Iron | Lead |
|---|---|---|---|---|---|
| | | | | | |
| Cd $K_{\alpha 1}$ | 23,17 keV | 14,46 cm | 8,20 mm | 0,70 mm | 77,30 µm |
| Mo $K_{\alpha 1}$ | 17,48 | 6,06 | 3,60 | 0,31 | 36,70 |
| Cu $K_{\alpha 1}$ | 8,05 | 5,51 mm | 0,38 | 36,40 µm | 20,00 |
| Ni $K_{\alpha 1}$ | 7,48 | 4,39 | 0,31 | 29,80 | 16,60 |
| Fe $K_{\alpha 1}$ | 6,40 | 2,72 | 0,20 | *164,00 | 11,10 |
| Cr $K_{\alpha 1}$ | 5,41 | 1,62 | 0,12 | 104,00 | 7,23 |
| S $K_{\alpha 1}$ | 2,31 | 116,00 µm | 14,80 µm | 10,10 | 4,83 |
| Mg $K_{\alpha 1}$ | 1,25 | 20,00 | 7,08 | 1,92 | 1,13 |
| F $K_{\alpha 1}$ | 0,68 | 3,70 | 1,71 | 0,36 | 0,26 |
| N $K_{\alpha 1}$ | 0,39 | 0,83 | 1,11 | 0,08 | 0,07 |
| C $K_{\alpha 1}$ | 0,28 | *13,60 | 0,42 | 0,03 | 0,03 |
| B $K_{\alpha 1}$ | 0,18 | 4,19 | 0,13 | 0,01 | 0,01 |

$Edge_{C\text{-}K}$ = 0.2842 $Edge_{Fe\text{-}K}$ = 7.112

# Information obtained by XRF measurements

✓ **Qualitative**

- **Elements present in the sample**
  - ➢ **Distribution of elements in the sample** (**mapping/scanning**, μ-beam/m-beam)
- **Semi-quantitative approach** (counts of peak areas, ratio of counts)

✓ **Quantitative**

- **Determination of elements' concentrations** (mass fraction μg/g, areal density μg/cm$^2$)
- **Determination of layers' thickness and density** (Angle-Resolved XRF)

# Qualitative analysis

**The information about the elements, their distribution and counts is enough for the study**

**The sample is not homogeneous** (on surface and/or in depth) **and cannot be prepared homogeneous** (cultural heritage, archaeology). The distribution of elements (also in underlying layers) is an extremely useful information

**The distribution of elements in the sample is the object of the study**, and the sample should not be homogenized (i.e., distribution of heavy elements in plants used for phytoremediation)

# Quantitative analysis

## Determination of elements' concentrations

**As an example, in the case of environmental studies, the qualitative analysis is not enough. It is important to know which toxic elements are present in the sample but also at which level**

The sample must be prepared to be homogeneous in surface and in depth

The mass, area and thickness of sample should be known

**Sample preparation is crucial and can be**, when not preformed properly, **one of the major cause of inaccuracy**

## Determination of layers' thickness and density

The layer thickness, composition and density should be homogeneous

# Sample preparation

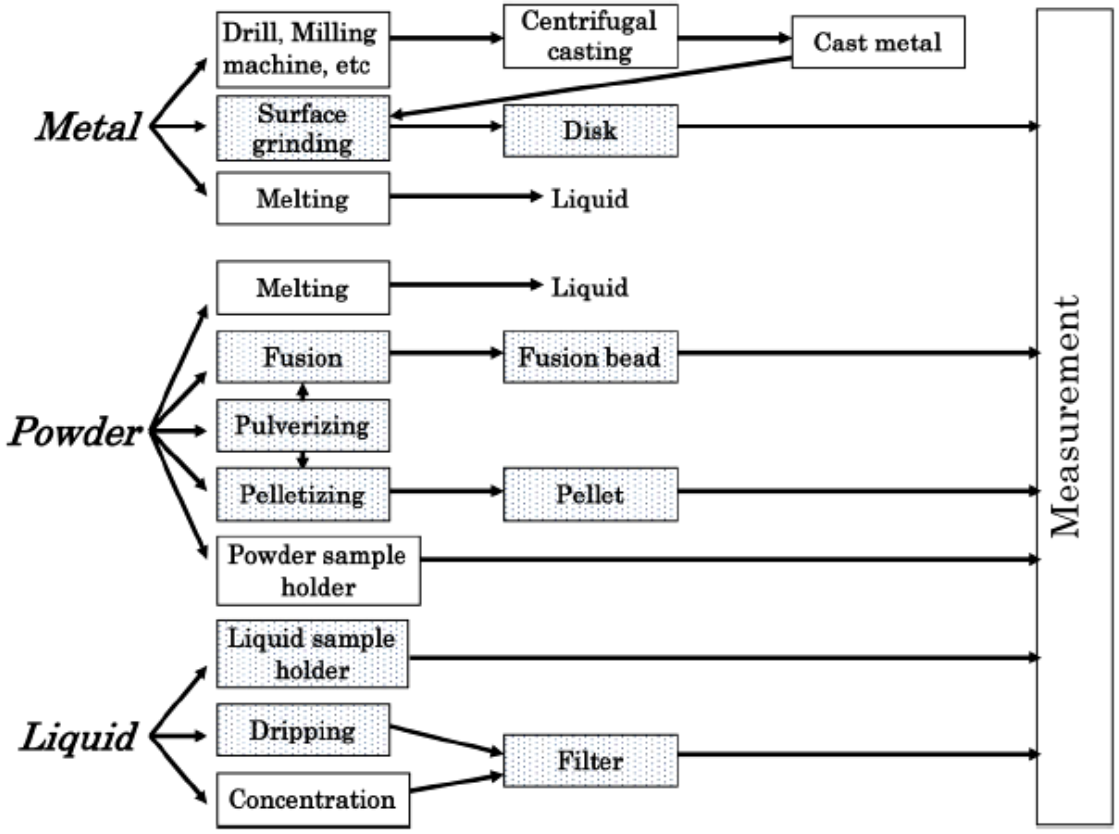


Yamada, 2014, *Sample preparation for XRF*, Rigaku Journal

# Quantification: linear calibrations

Change in response due to change in elemental concentration

Typically, quantification is performed calibrating the system using reference materials with similar matrices and different levels of the elements of interest

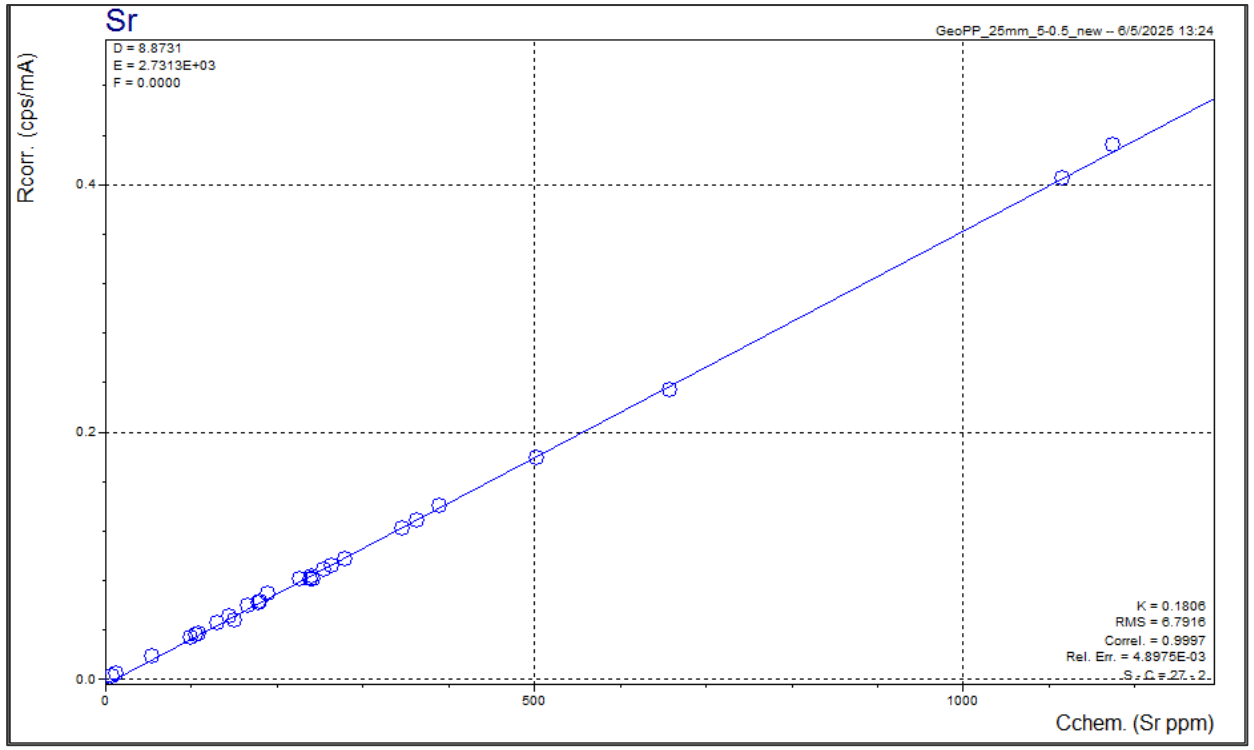


Sr sensitivity after correction, obtained with a secondary target ED-XRF spectrometer using Mo target

In case of matrix effects, the intensities of the peaks should be corrected (fundamental parameters, alpha coefficient, Compton normalization,…)

At synchrotrons, being the primary beam much easier to be described and the set-up features well-known, for some kind of samples the quantification can be performed with a full fundamental parameters approach

# Software for spectra deconvolution

| | QXAS | WinQXAS | PyMCA | WinAxil | bAxil |
|---|---|---|---|---|---|
| **Released by** | IAEA | IAEA | ESRF | Canberra | BrightSpec |
| **Availability** | Free upon request | Free upon request | Free download | $$$$ | $$$$ |
| **Operating Environment** | DOS [(a)] | Win 95 | Win 10 | Win 95-XP | Win 10 |
| **Multiple ROIs [(b)]** | No | Yes | No | No | No |
| **Scatter peaks fit** | Basic models | Basic models | No | Advanced | Advanced |
| **Spectrum format conversion** | Old formats<br>*.asc (ASCII)<br>*.spe (QXAS) | *.asc (ASCII)<br>*.spe (QXAS) | Different options | Multiple Canberra & Ortec, *.asc, *.spe | *.asc, *.spe, *.spc, *.txt, *.csv, *.mps, *.xml, *axml |
| **Batch run** | Yes | No | Yes | Yes | Yes |
| **Quantitative tools** | Multiple | Elemental sensitivity | Fund. Par. | Elemental sensitivity<br>Fund. Par. | No |

(a) Possibility of running on DOS Box for Windows

(b) Capable of selecting multiple Region of Interest for fitting

# Examples of experiments performed at the multipurpose joint IAEA-Elettra XRF beamline at Elettra Sincrotrone Trieste (now dismantled)


# Beamline and end-station

**Beamline**

| Source | **Bending magnet** |
|---|---|
| Flux | $10^{10}$ph/s (at 5 keV for 2.0 GeV, at 10 keV for 2.4 GeV) (Si 111) |
| Spot size | **250 x 100 (H x V) µm²** |
| Beam divergence | < 0.15 mrad (at exit slits) |

**End-station**

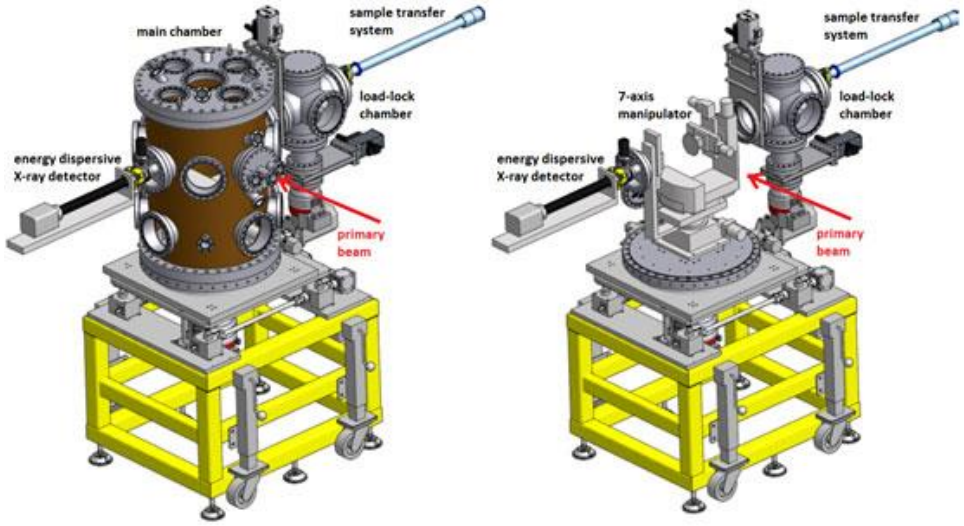


**Available detectors**:

- Diamond detector for $I_0$
- SDD detector for **XRF** (different variants) and **XAS** (in fluorescence geometry)
- Photodiodes for **XAS** in transmission geometry
- Photodiodes with 100 and 200µm slits and SDD for **XRR**

- Sample can be moved in various directions/ orientations with respect to the exciting X-ray beam or with respect to the detectors.
- Ultra Thin Window (UTW) Bruker Silicon Drift detector (30 mm², FWHM 131 eV @ Mn-Ka), Si photodiodes

# IAEA Coordinated Research Project

- **Materials Science**: Structured materials for energy storage and conversion technologies
- **Nanomedicine - Biosensing technologies**
- **Environmental monitoring** (air particulate matter, water)
- **Biological:** Elemental distribution/ speciation on plant organ (leaves, roots, shoots, seeds, etc.)
- **Cultural Heritage –preventive conservation**
- **Food products security – Authenticity**
- **Determination of X-Ray Fundamental Parameters**

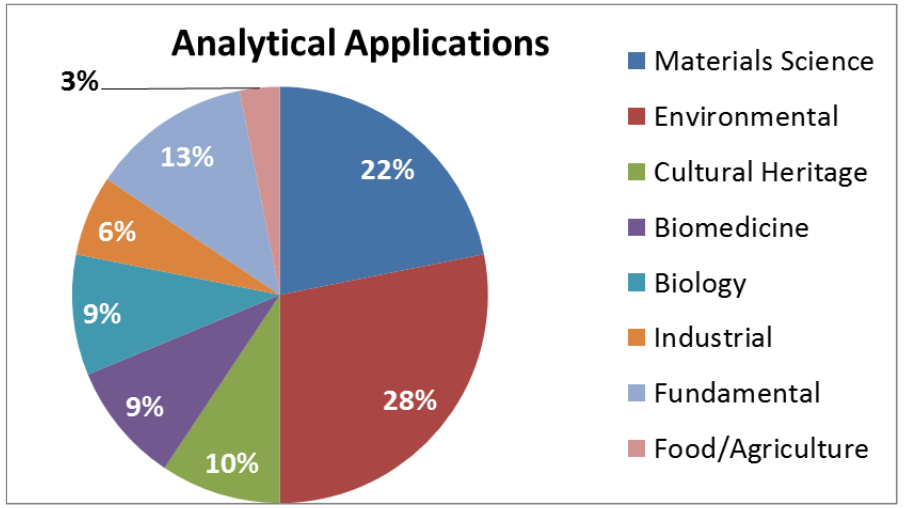


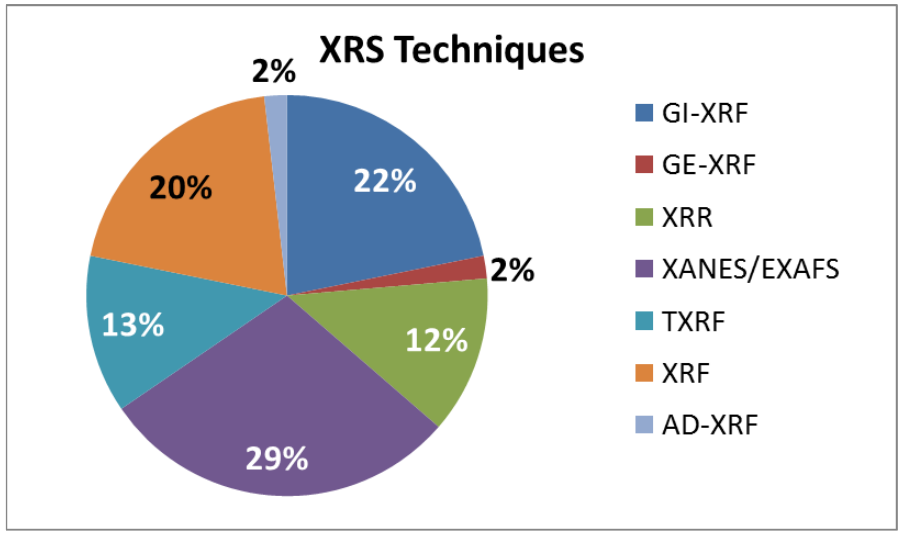

# Geometries and techniques

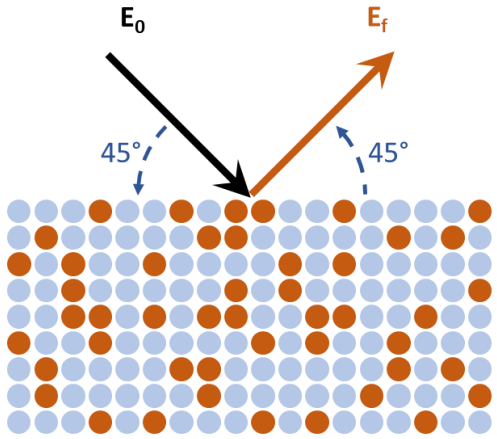


**Standard 45°/45° - XRF**

Elemental characterization

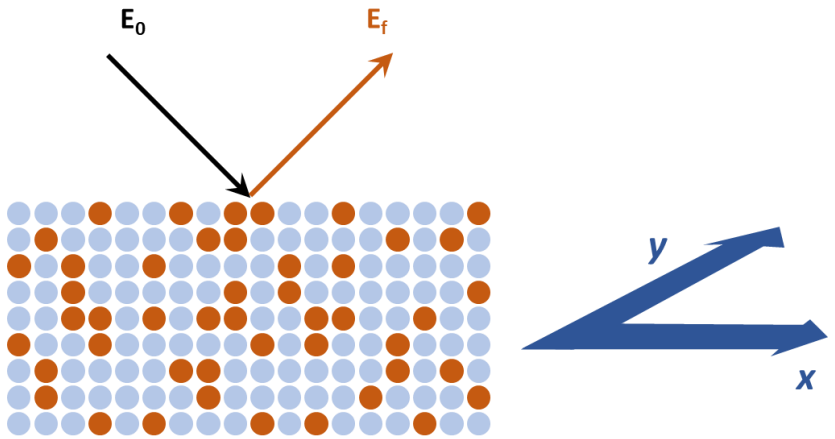


**micro - XRF**

Mapping

X-ray Absorption
Spectroscopy (on hot spots)

# Grazing angle geometries

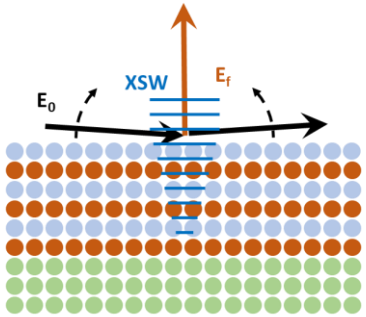


Grazing Incident - XRF

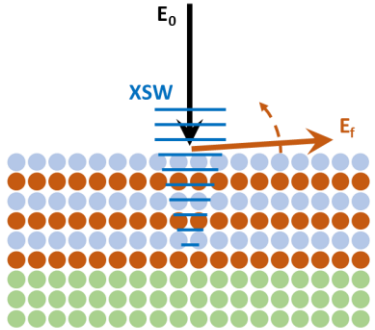


Grazing Emission - XRF

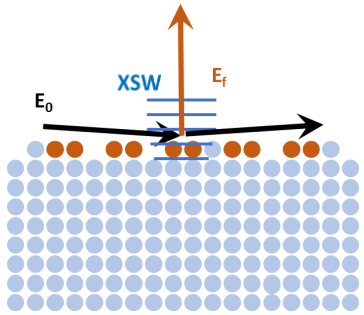


Total reflection - XRF

Depth profiling measurements

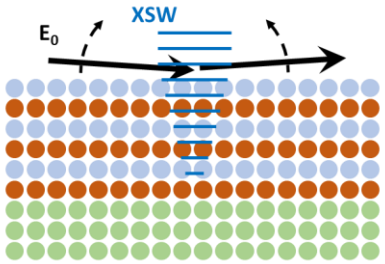


X-Ray Reflectometry

Trace element analysis
Surface contamination

X-ray Absorption Spectroscopy
(in TXRF geometry)

# Se and Hg in edible mushrooms

**K. Vogel-Mikuš [1], P. Kump[2], I. Arčon[3]**
[1] Biotechnical faculty, University of Ljubljana, [2]Jozef Stefan Institute,
[3] University of Nova Gorica

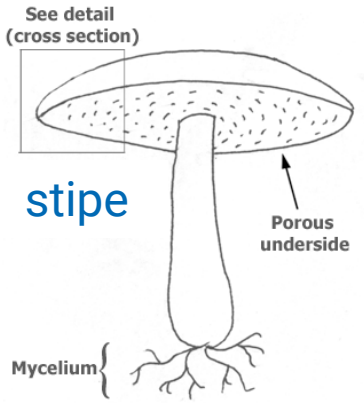


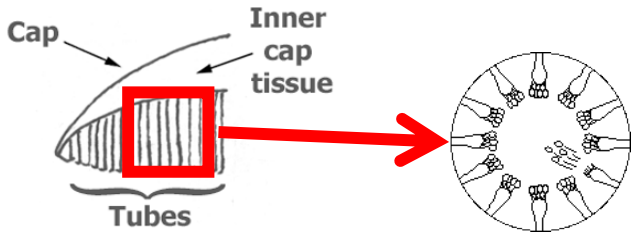


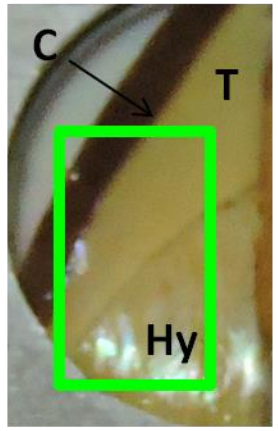


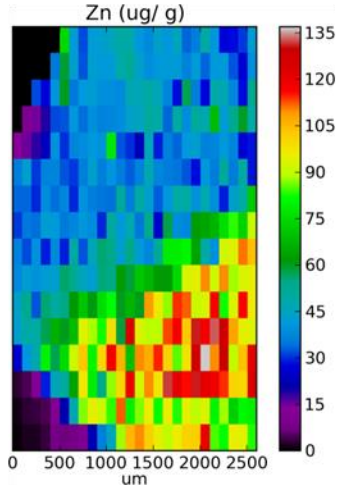


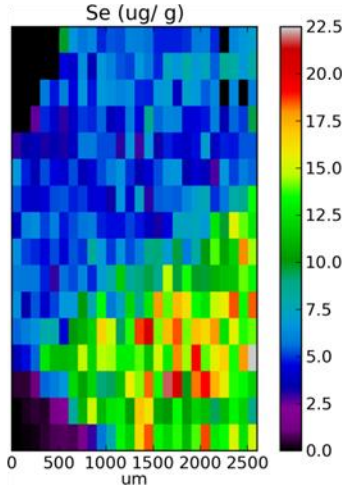


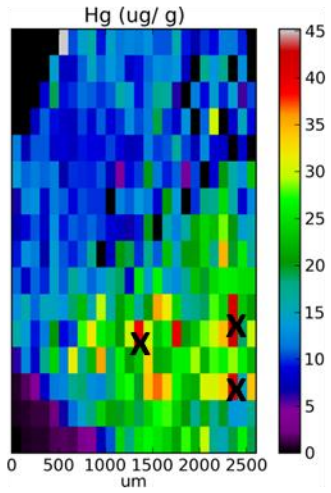


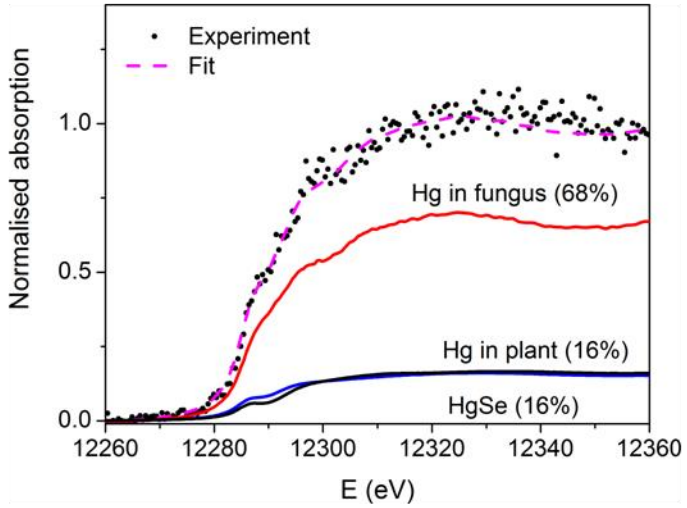


Hg is bound to tetra-cysteine proteins (metallothioneins). These proteins are digested by enzyms in the stomach and Hg is released and absorbed in our body.

# Analysis of gold samples

## Absorption edges of Pt and Au

| | Pt | Au |
|---|---|---|
| Z | 78 | 79 |
| L1 (keV) | 13.88 | 14.353 |
| L2 (keV) | 13.273 | 13.734 |
| L3 (keV) | 11.564 | 11.919 |

Pt Lα: 9.44 keV

Au Lα: 9.71 keV

**Synchrotron XRF spectra of pure (99.99%) thick (thickness 25 μm) gold samples**

**X-ray Resonant Raman Scattering (RRS)**

**$E_0$ = 11600 eV @Elettra**
pure gold spectrum vs.
gold alloy with 0.15% Pt (Au: 65.56%, Cu: 25.21%, Ag: 9.08%) and vs.
a different certified alloy of similar composition without Pt
11600 eV > Pt(L3) = 11564 eV

Courtesy of A.G.Karydas, (National Center for Scientific Research "Demokritos", Greece)

Incident energies employed: 11600, 11650, 11700, 11800 eV

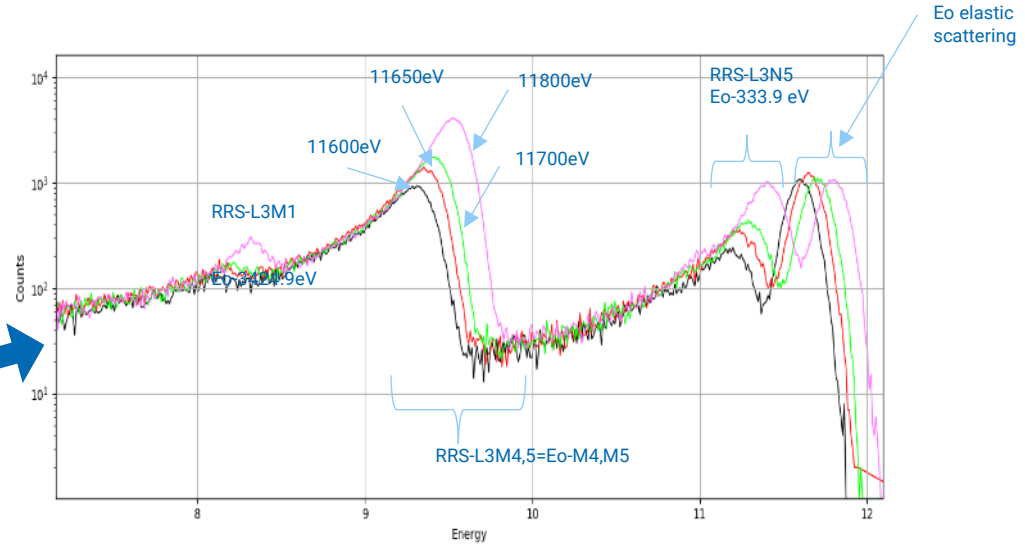


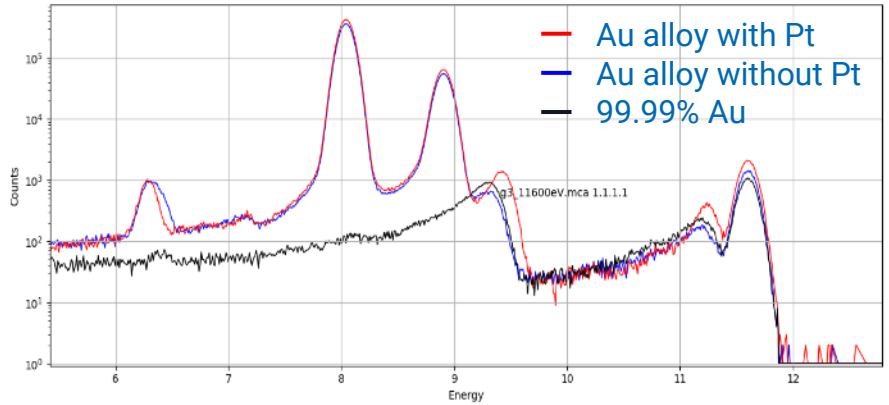

# GIXRF: C/Ti double layer

Prepared and characterized by AXO Dresden


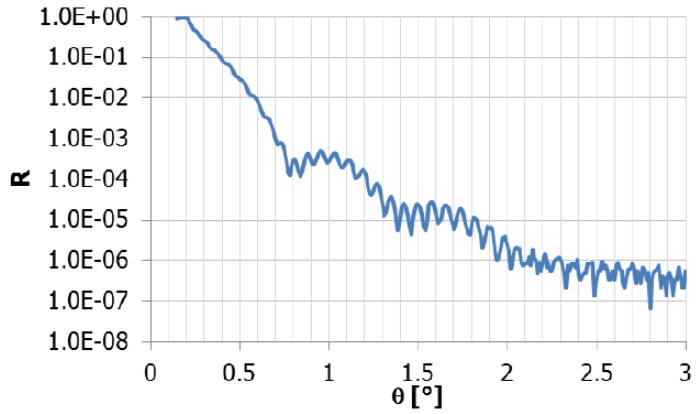


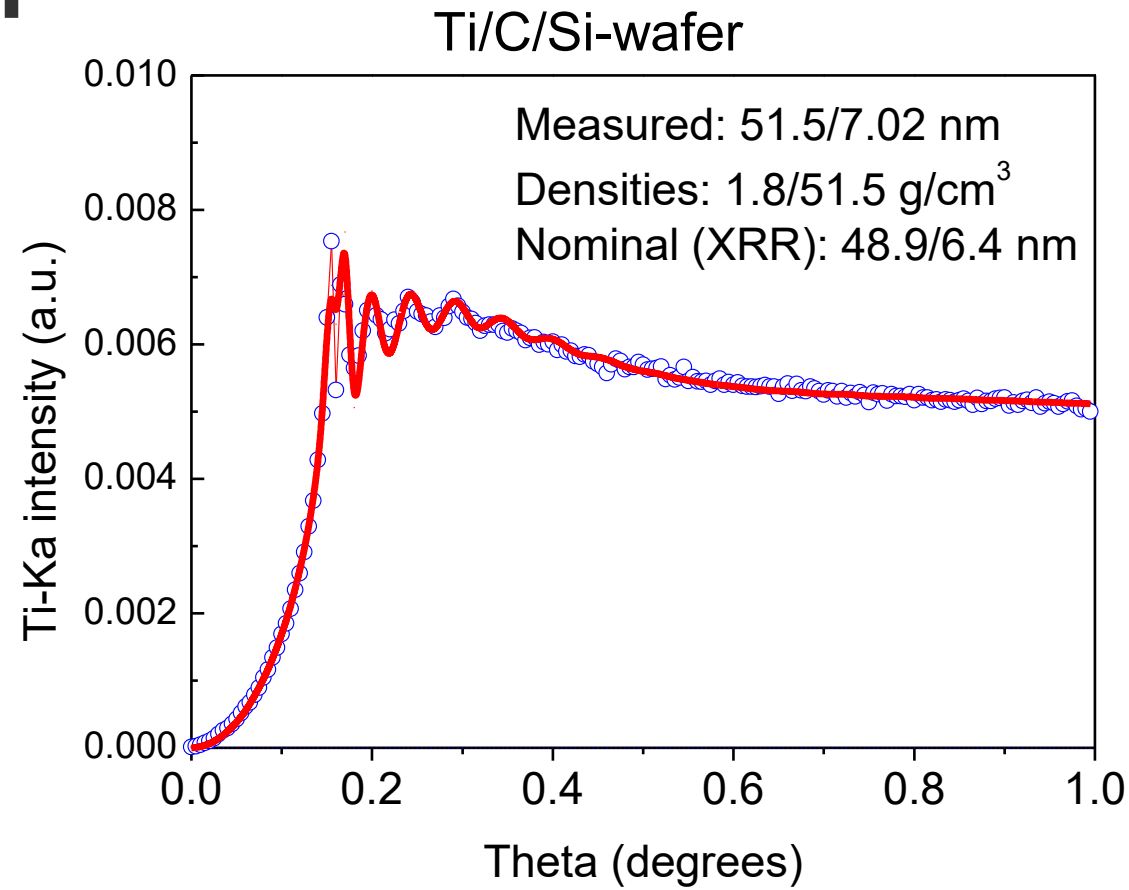


| | Fit | Nominal |
|---|---|---|
| Ti (nm) | 7.0 | 6.4 |
| C (nm) | 51.5 | 48.9 |

# W/B4C multilayered (x15) thin film

Multilayered sample, prepared by the Ramanna Center for Advanced Technology, Indore, India

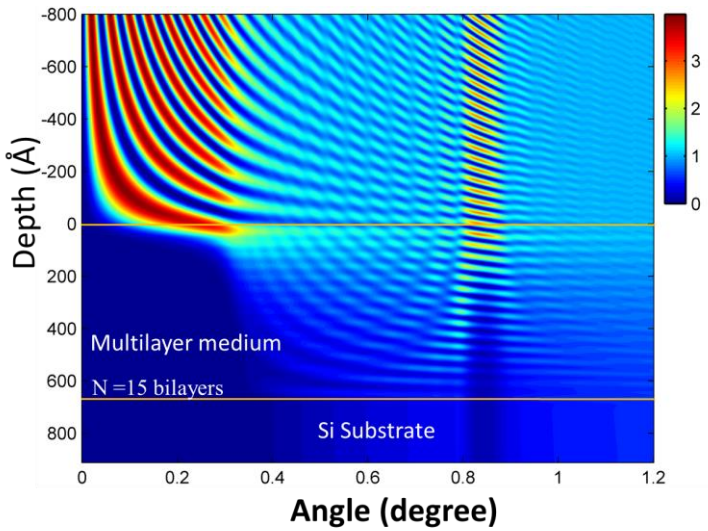


Electric Field Intensity (Normalized)

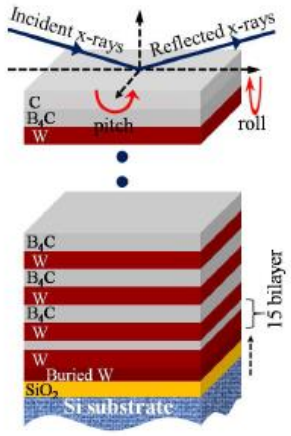


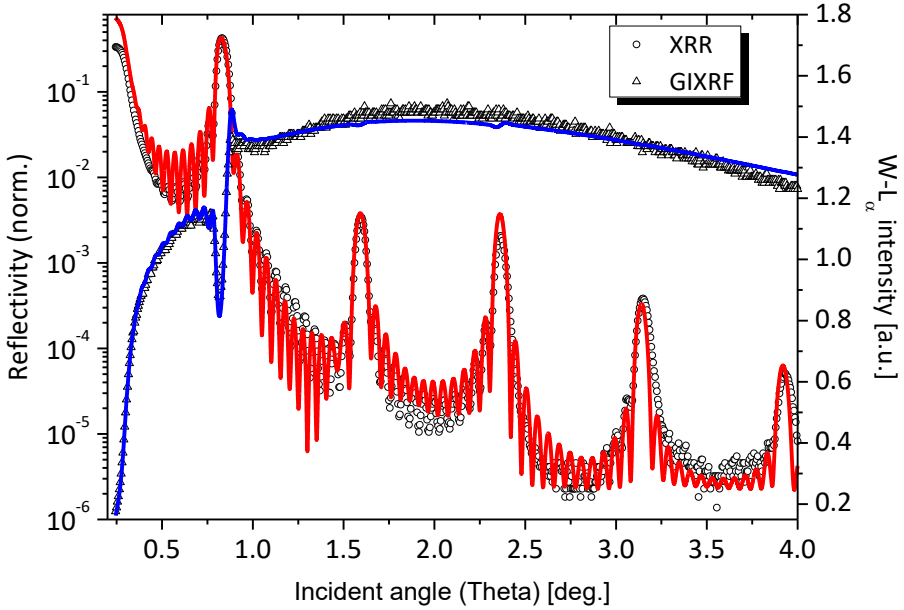


good agreement with previous analyses performed at the BL-16 beamline of Indus II

| | | 'B$_4$C'/'W' multilayer | | |
|---|---|---|---|---|
| Layer Material | Periodicity | Thickness (nm) | Roughness (nm) | Density (g/cm$^3$) |
| B$_4$C | 14 | 1.9 ± 0.1 | 0.2 ± 0.1 | 2.10 ± 0.2 |
| W | | 2.4 ± 0.2 | 0.3 ± 0.1 | 16.0 ± 0.2 |
| B$_4$C | 1 | 2.1 ± 0.6 | 0.45 ± 0.2 | 2.3 ± 0.2 |
| W | | 3.6 ± 0.3 | 0.55 ± 0.2 | 15.5 ± 1.0 |
| SiO$_2$ | 1 | 2.0 ± 0.3 | 0.5 ± 0.2 | 2.0 ± 0.3 |

# Zn speciation in fractionated APM

**9-stage May-type cascade impactor**

Sampling of size fractionated aerosol, down to 0.07um size 20-3200 L of air

Deposited particles form a stripe of 200-500 µm width on the 20x20 $mm^2$ Si wafer

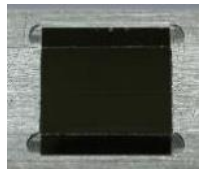

**Sample geometry well suited to SR-TXRF-XANES investigations!**

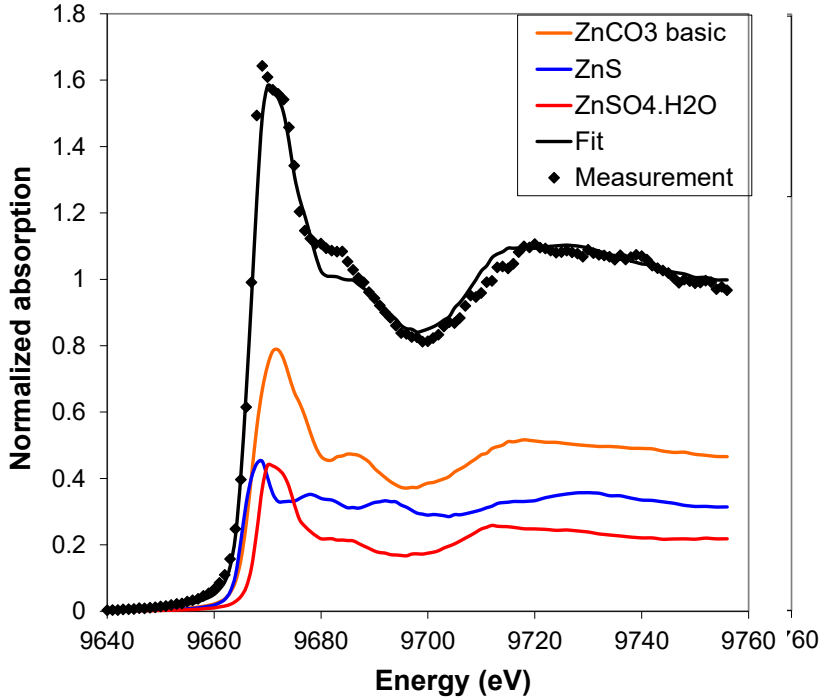


Sample: Paks (Hungary), 0.3–0.6 µm
Zn content: 74 ng/m3 (28.5 ng on 20 mm strip)

38% $ZnSO_4$, 40% ZnS, 23% Zn in glass*

Main source: **Iron smelter**

Sample: Budapest (Hungary), 0.15–0.3 µm,
Zn content: 239 ng/m3 (84 ng on 20 mm strip)

47% $ZnCO_3$, 32% ZnS, 22% Zn in glass*

Main source: **Burning of painted wood**

**J. Osan,** Environmental Physics Department, Centre for Energy Research, Budapest, Hungary

*Self-absorption correction as described in: Osán J et *al*., Spectrochim Acta Part B 65 (2010) 1008-1013

# Joint IAEA-Elettra training


**5 editions from 2019 to 2025**

Young scientist with no or limited experience in synchrotron light experiments to participate in extended hands-on experiments and training at different beamlines, as well as to learn how to write successful proposal applications to be able to secure beamtime for themselves

**Joint IAEA-Sesame training**

The training **will be announced soon** and will be held in November 2026

*ICTP School on Synchrotron Light Sources and Their Applications* (12 - 23 January 2026)

# Thank you for your attention!

a.migliori@iaea.org